

4-27
CONFIDENTIAL

Copy -223
RM L51D17

NACA RM L51D17

53-34-19

NACA

0143851

TECH LIBRARY KAFB, NM

RESEARCH MEMORANDUM

AN INVESTIGATION OF FOUR WINGS OF SQUARE PLAN FORM

AT A MACH NUMBER OF 6.86 IN THE LANGLEY

11-INCH HYPERSONIC TUNNEL

By Charles H. McLellan, Mitchel H. Bertram,
and John A. Moore

Langley Aeronautical Laboratory
Langley Field, Va.

~~CONFIDENTIAL~~
This document contains classified information affecting the National Defense of the United States within the meaning of the Espionage Act, USC 50:31 and 32. The transmission or the revelation of its contents in any manner to an unauthorized person is prohibited by law.
Information so classified may be imparted only to persons in the military and naval services of the United States, to civilian officers and employees of the Federal Government who have a legitimate interest therein, and to United States citizens of known loyalty and discretion who of necessity must be informed thereof.

NATIONAL ADVISORY COMMITTEE
FOR AERONAUTICS

WASHINGTON
June 29, 1951

CONFIDENTIAL

319.98/13

52-65

7243

Classification change 1-a (or changed to) **CONFIDENTIAL**
By Authority of **NASA Technical Office memo**
(OFFICER AUTHORIZED TO CHANGE)
92 15 Nov 55

By.....

MS
GRADE OF OFFICER MAKING CHANGE)
10 Apr 61
DATE



0143851

NACA RM L51D17

~~CONFIDENTIAL~~

NATIONAL ADVISORY COMMITTEE FOR AERONAUTICS

RESEARCH MEMORANDUM

AN INVESTIGATION OF FOUR WINGS OF SQUARE PLAN FORM
AT A MACH NUMBER OF 6.86 IN THE LANGLEY
11-INCH HYPERSONIC TUNNEL

By Charles H. McLellan, Mitchel H. Bertram,
and John A. Moore

SUMMARY

The results of pressure-distribution and force tests of four wings at a Mach number of 6.86 and a Reynolds number of 980,000 in the Langley 11-inch hypersonic tunnel are presented. The wings tested had a 4-inch square plan form, a 5-percent maximum thickness, with diamond, half-diamond, wedge, and half-circular-arc sections.

Large deviations of the measured pressures from those predicted by the inviscid theory were found at the leading edge of the wing and just back of sudden changes in surface slope. These pressure deviations were attributed to a rapid growth of the laminar boundary layer at the high test Mach number. The effect of boundary layer on the pressures on a flat surface parallel to the stream was in good agreement with theoretical results for which the boundary layer was assumed to be laminar. Separation effects similar to those normally encountered at lower Mach numbers were also present at the rear of the airfoils.

The effects of the departures of the pressures from those predicted by inviscid theory over the various parts of the airfoils tended to compensate each other; thus the wing aerodynamic characteristics due to pressure forces can be predicted with reasonable accuracy by two-dimensional inviscid theory at a Mach number of 6.86. At high angles of attack the experimental lift and drag results from force measurements were somewhat lower than the value given by the inviscid theory because of separation and tip effects. At low angles of attack, the skin friction must be taken into account in calculating the total drag coefficients and lift-drag ratios of wings.

The two wings having symmetrical airfoil sections (the diamond and wedge sections) had the highest maximum lift-drag ratios from pressure

~~CONFIDENTIAL~~

PERMANENT
RECORD



52-65

measurements and the half-circular-arc section had the lowest. The differences, however, were small when skin friction was included, the over-all maximum lift-drag ratio being close to 6 for all the wings tested.

INTRODUCTION

In evaluating the performance of contemplated missiles at high supersonic (hypersonic) Mach numbers, it has been necessary up to this time to use theoretical results without experimental verification. The opportunity for an experimental investigation of wings and bodies in hypersonic flow was presented with the completion of surveys of the flow in a two-dimensional, single-step nozzle in the Langley 11-inch hypersonic tunnel.

The results of an investigation of the aerodynamic characteristics of four wings of square plan form at a Mach number of 6.86 and a Reynolds number of 980,000 based on the 4-inch wing chord are presented in this paper. These wings were 5 percent thick and had diamond, half-diamond, half-circular-arc, and wedge airfoil sections. The wings with the diamond and wedge airfoil sections were tested through a range of angle of attack from 0° to about 25° , while the wings with the half-diamond and half-circular-arc airfoil sections were tested through a range from about -25° to 25° . Both pressure and force measurements were made and compared with theoretical results.

SYMBOLS

b	span
C_D	wing drag coefficient
C_L	wing lift coefficient
C_f	wing skin-friction coefficient
c_n	section normal-force coefficient
C.P.	center-of-pressure location in chord lengths
D	drag
L	lift

M	free-stream Mach number
P_1	free-stream static pressure
P_2	surface static pressure
P_b	base pressure
R	Reynolds number based on free-stream conditions and wing chord
x	distance along chord measured from leading edge
y	distance along span measured from midspan
α	angle of attack of airfoil or flat plate

DESCRIPTION OF APPARATUS AND MODELS

Tunnel.— The tests of this investigation were conducted in the Langley 11-inch hypersonic tunnel. This tunnel is of the blowdown type and has a test duration from 60 to 90 seconds, depending on the test configuration. A description of the tunnel is given in reference 1. As shown in reference 2, the flow in the tunnel test section with the two-dimensional nozzle used during this investigation is sufficiently uniform for model testing in the central core of the stream about 5 inches square in cross section. The Mach number in this region is about 6.86.

Models.— The wings tested, which are shown in figure 1, incorporated four airfoil sections - the diamond, half-diamond, wedge, and half-circular-arc. All the wings were of 4-inch chord, were 5 percent thick, and had an aspect ratio of 1. Two sets of models were used - one designed for force measurements and the other for pressure measurements. The models, which were made of steel, were accurately machined and polished, and the surfaces and edges were maintained in good condition during the tests by periodic polishing. Special efforts were made to obtain sharp leading and trailing edges and the thickness of these edges was between 0.001 and 0.002 inch. An additional model having a 20° wedge angle was included in order to obtain supplementary pressure data near the leading edge.

Model support system.— The models were mounted on the support stings shown in figure 1. The stings were attached to a diamond-shaped support strut which spanned the tunnel vertically just downstream of

the test section. (See references 1 and 2.) The pressure models were attached to their sting supports by means of a swept offset arm affixed to the under surface of the models so that the upper surface where the pressures are measured was free from any obstruction. The angle of attack of the pressure models was varied by rotating the offset arm to predetermined settings.

The force models were attached to the force-model support stings by a 6.7° included angle cone with the 0.5-inch-diameter base about 1.5 inches downstream of the trailing edge of the wing. The cone was affixed directly to the rear surface of the model with the cone axis parallel to the wing chord line. (See fig. 1.) The cone for the wedge model was attached to the blunt trailing edge. With the three-component force balance, the angle of attack was varied by using bent sting attachments just back of the cone attachment. This part of the sting just back of the cone was attached directly to the front of the sting balance and was shielded from the air stream. The angle of attack for the two-component balance was varied by rotating the forepart of the sting housing the balance.

Instrumentation of pressure models.- Pressure orifices were located along the chord of the model at the midspan section, as shown in figure 1. On most models, it was difficult to install a pressure orifice any closer to the leading or trailing edge than about 4 to 6 percent of the chord because of the thinness of the model. The leading edge of the wedge airfoil was so thin that the most forward orifice location was limited to about 12.5 percent of the chord from the leading edge.

Additional chordwise rows of orifices were installed in the wing having the diamond airfoil section at spanwise stations 31, 62.4, and 80.4 percent semispan from the center span. Orifices were also installed in the base of the wing having the wedge airfoil section. These were installed at 14, 37.6, 53, 71, and 95.6 percent semispan from the midspan section and halfway between the upper and lower surfaces.

In order to obtain pressures near the leading edge of a flat surface parallel to the stream, the special model was used which had a leading-edge included angle of 20° . This relatively large angle allowed orifices to be installed within about 0.125 inch from the leading edge. The large angle on the under side has no effect on the pressures on the upper side.

Because of the thinness of the model, it was impractical to conceal inside the model the tubing which connected the orifice to the measuring instrument. A 0.040-inch inside-diameter tube formed the pressure orifice on one side and projected through the opposite surface where it

was joined to a 0.060-inch inside-diameter (0.090-inch outside-diameter) tubing as shown in figure 1. At the high Mach number used in this investigation, the presence of the tubing on one surface did not affect the pressures on the opposite surface except possibly slightly at the trailing edge and on the base pressure of the wedge model.

The pressures were measured by means of the bellows-type six-cell recording units, described in reference 1, which convert the deflection of a bellows into a rotation of a small mirror reflecting a beam of light to a moving film; thereby a time history of the pressure is given.

Instrumentation of the force models.- The forces acting on the force models were measured by means of two strain-gage balances which were also part of the sting support for the model. Nearly all the force tests were made by using the three-component balance, shown in figure 2, which was designed to measure lift, drag, and pitching moment. Pitching moments, however, were unreliable because of uneven heating of the pitch beams and thus were not used.

The instrumentation of the strain gages on the balance was such that temperature changes did not affect the calibration, provided that the whole balance was at a nearly uniform temperature. In order to reduce the amount of heating during tests, the exterior of the balance shield was coated with a porcelain insulation. The lift and drag components of this balance were designed for a maximum measurable load of 20 and 10 pounds, respectively, with an accuracy of 0.1 pound in lift and 0.05 pound in drag. In practice, this accuracy was not always realized because of uneven heating effects. These heating effects were somewhat erratic - at times being negligible and at other times having a moderate effect on the tare readings taken before and after the run.

A two-component strain-gage balance was designed to measure the lift and drag more accurately at low angles of attack than with the three-component balance. This balance, which is shown in figure 3, was designed for a maximum normal load of 5 pounds and a maximum chordwise load of 1 pound; in each case, the balance was designed to give an accuracy of 1/2 percent of the maximum load. The effects of heating on this balance, however, were much greater compared to the design accuracy than that experienced on the three-component balance, which somewhat reduced the relative accuracy.

Schlieren system.- The schlieren photographs presented in this paper were taken by means of the schlieren system described in reference 1. Some of the photographs were taken with an exposure of 1/150 second and others with a flash of a few microseconds' duration. A horizontal knife-edge position was used for all photographs. The greatest limitation on the sensitivity of this schlieren system is the

heating effect on the windows. Since the stagnation temperature of the air in the tunnel was about 730° F for most tests, the inner surface of the glass windows became heated so that dark, nearly horizontal bands appeared in the schlieren photographs. In order to minimize this effect, most of the photographs used were obtained during the first part of the runs. The Mach number may, therefore, be as much as 3 percent lower than the calibrated value. The variation of Mach number with time is discussed in the following section.

OPERATING CONDITIONS

The tests were conducted at a stagnation pressure of approximately 25.5 atmospheres and a stagnation temperature of about 730° F. The high stagnation temperature is necessary to maintain the air temperature in the test section above the normal static liquefaction temperature. With the high stagnation temperature, a warpage of the first minimum of the nozzle takes place during the runs and results in a variation with time in the test section Mach number of about 3 percent. (See reference 2.) By using only the test results at 60 seconds from the beginning of the runs, which is the same procedure used in the nozzle calibration presented in reference 2, the effect of the varying Mach number was practically eliminated.

The Reynolds number for these tests was about 980,000 based on a 4-inch chord. It is interesting to note that this Reynolds number corresponds to a wing with a 4-foot chord flying at the test Mach number at an altitude of about 120,000 feet or a 2-foot chord at an altitude of about 107,000 feet.

DATA ACCURACY

Tunnel flow characteristics.- The test section of the single-step nozzle used in this investigation had a central core of reasonably uniform flow about 5 inches square in cross section. The Mach number variation of the flow in the part of the core in which the wings were tested ranged from about 0.7 percent above to 0.2 percent below the mean Mach number of 6.86. The flow at the center of the test region was essentially parallel to the tunnel axis, whereas at the extremes of the test region the flow deviated about one-fourth degree in the vertical plane away from the horizontal plane passing through the center line of the nozzle. In the horizontal planes in the test region, the deviation of the flow was negligible.

Angle of attack.— The differences between the support systems used for the pressure tests and for the force tests necessitated two different methods of measuring angle of attack. For the pressure tests, the use of a rigid model support and lack of any significant deflections under any test conditions simplified angle-of-attack measurements. In this case, angle of attack was determined before the test run by measuring the height of the leading and trailing edges of the model from the bottom surface of the nozzle which, at the test section, is a plane surface. The accuracy of measurement of angle of attack by this method is within 0.2° .

The use of a relatively flexible support in tests of the force models made necessary the determination of the angle of attack during the test run. This angle was determined by measurements of the model angle with respect to the reference lines on the schlieren photographs. The accuracy of this method was also limited to about 0.2° .

Pressure measurements.— The pressure cells used in this investigation have an accuracy of $1/2$ percent of the full-scale reading. Full-scale deflection, however, was seldom attained. In the most sensitive of the pressure cells, the free-stream pressure was about one-fourth of the full-scale deflection; the accuracy in this case was about ± 2 percent.

In the calculation of the ratio $\frac{P_2 - P_1}{P_1}$ using pressures measured by the cells, the probable maximum error including the effect of possible error in angle-of-attack setting is about ± 0.07 when the ratio is zero, about ± 2 percent as the ratio approaches -1 , and about ± 3 percent at very large values. The coefficients computed from these pressures have an accuracy of about ± 0.003 in lift and ± 0.002 in drag at low angles of attack while at the highest angles of attack tested, the probable maximum error is ± 0.008 in lift and ± 0.002 in drag.

Force measurements.— The errors in force coefficients arise mainly from errors in Mach number and static-pressure determination and from the force-balance sensitivity. Errors due to heating effects were reduced by discarding the results of tests in which excessive differences were noted between the tare readings before and after the test. The force measurements on the force models included the force due to the conical support and its interference effects. Corrections to the lift and drag due to aerodynamic forces on the unshielded portion of the conical support were applied to the wing force-test results. These corrections were based on theoretical results for complete cones with limited experimental checks. No attempt was made to determine the

effects of interference but these are believed to be small since the area affected by the shocks from the support constitutes less than 5 percent of the wing surface area.

At low angles of attack, the sensitivity of the balance was the predominant factor. For this condition, the probable maximum error in lift and drag coefficients is about ± 0.003 and ± 0.0015 , respectively. At high angles of attack, the accuracy of Mach number and static pressure measurement were the important factors. At the highest test angle, the probable maximum errors in lift and drag coefficients were about ± 0.008 and ± 0.004 , respectively.

PRESENTATION OF RESULTS

Pressure Measurements

Chordwise pressure distribution.— The pressures over the midspan section of the wings at various angles of attack are presented in figures 4 to 8. The pressures measured at each orifice are presented as the nondimensional pressure rise $\frac{P_2 - P_1}{P_1}$ where P_2 is the local static pressure and P_1 is the free-stream pressure. This ratio has a value of zero when the local surface pressure is equal to the stream static pressure and has a value of -1 at zero absolute pressure on the surface.

Theoretical two-dimensional pressure distributions over the models are also presented on these figures. These distributions have been calculated by using the Prandtl-Meyer expansion equations and the oblique shock relations. For the diamond, half-diamond, and wedge airfoil sections, these relations give exactly the same results as the shock and characteristics theory. For the half-circular-arc airfoil at the test Mach number, the differences in pressure distributions calculated by the Prandtl-Meyer equations and the characteristics theory with rotational flow are negligible.

In order to simplify the presentation of the results, the pressures on the flat surface of the half-circular-arc wings have not been included; however, the tests gave the same results for the flat sides of both the half-diamond and half-circular-arc wings.

The results of a study of the pressure distribution over a flat surface parallel to the stream are presented in figure 9. The experimental pressures were obtained from several of the models having flat surfaces and from the model with a 20° wedge angle.

The theoretical pressure distribution plotted in figure 9 is based on the assumption that the boundary layer effectively changes the shape of the body by an amount equal to the displacement thickness of the boundary layer. In calculating the boundary layer, laminar flow with a linear velocity profile and a Prandtl number of unity along an insulated flat plate is assumed, and Sutherland's formula is used for the viscosity variation. A nearly linear distribution at high Mach numbers was predicted from theoretical considerations in references 3 and 4. The variation of the theoretical pressure distribution with distance along the chord, figure 9, however, is not very sensitive to the shape of the boundary-layer profile and considerable variation in the velocity profile could, therefore, be tolerated without changing the theoretical results significantly.

A schlieren picture showing the thick boundary layer over one of the wing models with the flat surface up and parallel to the stream is also included in figure 9 together with a schematic diagram of the model showing the boundary layer and upper surface shock.

Figure 10 presents the results of an investigation of the effect of the leading-edge thickness on the pressures at various distances from the leading edge of a flat surface parallel to the stream. These results were obtained by varying the leading-edge thickness of the 20° wedge from 0.001 to 0.008 of an inch. The thickness was varied by cutting off the leading edge normal to the upper surface.

Spanwise variation of pressure distributions and normal-force coefficients.— The chordwise pressure distribution at the four spanwise stations on the diamond airfoil are presented in figure 11 for an angle of attack of 10°. The theoretical pressure distributions are those given by the two-dimensional inviscid theory and are shown only for those portions of the surface that are theoretically two dimensional. Both the experimental and theoretical pressure distributions have been integrated to obtain the section normal-force coefficients which are presented in figure 12. The two-dimensional theoretical coefficients are included only as far outboard as the flow is theoretically two dimensional over the whole chord. In order to show the individual contribution of the upper and lower surfaces to the over-all section lift coefficients, these surfaces are shown separately.

Base pressure on the wedge airfoil.— Base-pressure measurements on the wedge-section wing were made in order to complete the determination of the section characteristics of this wing. Base pressures were measured at five spanwise locations to avoid interference effects due to the support strut. The variation of base pressure with angle of attack is presented in figure 13.

Wing Characteristics

Figures 14 to 21 present the aerodynamic characteristics (C_L , C_D , center of pressure, and lift-drag ratio) of the four wings. Test results from both pressure measurements and force measurements are included. The coefficients obtained from pressures actually represent the section coefficients at the center of span and can be considered to represent the over-all coefficients only if the tip effects are neglected. The coefficients from the force tests, on the other hand, include the tip effect and are actually over-all coefficients of the wing.

The solid-line curves in figures 14 to 21 represent the two-dimensional theoretical coefficients obtained by integration of the theoretical nonviscous pressure distributions. A calculated skin friction has been added to the drag coefficients and the results are presented as dashed-line curves. The viscous drag coefficients have been calculated by making the same assumptions as were made for the calculation of the effect of the boundary layer on the pressure distribution over a flat plate parallel to the stream. The zero angle-of-attack friction drag coefficients for the diamond, half-diamond, wedge, and half-circular arc were 0.0028, 0.0030, 0.0029, and 0.0029, respectively. These values of the friction coefficients were corrected for a slight variation with angle of attack.

The theoretical curves in figure 18 are based on a base pressure on the wedge airfoil equal to one-half of the stream pressure which is roughly the value obtained from pressure measurements. No attempt was made to evaluate the base pressure theoretically. The variation in the coefficients due to changing the base pressure by an amount equal to one-half of the stream pressure in either direction would be very small and not noticeable in this figure. This variation in base pressure, however, has an appreciable effect on the lift-drag ratios for the wedge airfoil which are presented in figure 19. In this figure, the theoretical lift-drag ratios are presented for three values of base pressure even though the base pressures measured were approximately one-half of stream pressure.

Schlieren Photographs

Typical schlieren photographs of the flow about the wing with the diamond airfoil section are presented in figures 22 to 25. As these photographs were taken with the model mounted on the force balance, the trailing edge of the model is hidden by the sting mounting. The location of the trailing edge can be estimated by noting the break in the surfaces (at the maximum thickness) which occurs at the 50-percent-chord station.

DISCUSSION

Pressure Results

The pressure data of figures 4 to 7 show large deviation from the pressures predicted by inviscid theory. In addition to the usual departures of the measured pressures from those predicted by theory for supersonic flow in the region near the trailing edge and which are attributed to separation caused by an interaction between the boundary layer and the trailing-edge shock, the pressures also show large rises at the leading edges and just back of abrupt changes in the slopes of model surfaces. (See, for example, figs. 4, 5, and 6.) These pressure rises at the leading edges are evident even for the case of a flat surface parallel to the flow for which inviscid theory indicates no pressure rise.

The leading-edge pressure rise could conceivably be caused by either leading-edge thickness effects or by viscous effects, and both of these possibilities were investigated.

Effect of leading-edge thickness.— Pressure data obtained in tests of a wedge with the upper surface parallel to the flow show in figure 10 that at the most forward station on the wedge 0.12 inch downstream of the leading edge the pressure ratio $\frac{P_2 - P_1}{P_1}$ nearly doubles as the leading-edge thickness is increased from 0.001 inch to 0.008 inch. Since the thickness of the leading edges of all models tested did not exceed 0.002 inch, the pressure rise due to leading-edge thickness is small and cannot be considered the major cause of the pressure rise at the leading edge of the wings tested.

The boundary layer and its effect on the flow.— An analysis was made to determine the rate of growth of the boundary layer on a flat plate at a Mach number of 6.86 for laminar flow and a linear velocity profile. At a Mach number of 7, the calculated boundary-layer displacement thickness is about 10 times as thick as at a Mach number of 1 for equivalent Reynolds numbers. Pressure distributions calculated for the flat surface with boundary layer are in good agreement with the experimental data, figure 9. Shock boundary-layer interaction at the leading edge was neglected. This analysis has shown that the large pressure rise at the leading edge is primarily due to the very rapid growth of the boundary layers at high Mach numbers.

Further experimental verification of the large thickness of the boundary layer was obtained by means of schlieren photographs. This

thick boundary layer is apparent in the schlieren photographs in figure 9 which shows the flow about a wedge with the upper surface parallel to the air stream. Since the surface is parallel to the stream, the presence of the shock (fig. 9) is attributed to the boundary layer at the leading edge. The curve of the shock near the leading edge is due to the shape of the boundary layer as is depicted in the schematic representation of figure 9. After the leading edge the schlieren photograph shows the boundary layer as light and dark bands just above the model surface. The method of model support unfortunately prevented schlieren observation of the flow at the trailing edge.

Pressures greater than those predicted by theory also occur just behind abrupt changes in the slope of the surface such as at the maximum thickness on the diamond airfoil (fig. 4). The effect of the change in direction of the surface is not felt by the stream outside of the boundary layer for an appreciable distance back of the change in the surface slope. The schlieren picture of the diamond airfoil at 0.5° angle of attack (fig. 22) indicates that the point at which the flow outside of the boundary layer changes direction is about 5-percent chord downstream of the change in surface slope; in addition, the effect of the turning of the air outside of the boundary layer cannot be felt at the surface for an appreciable distance downstream of the point where the outside flow is deflected. The over-all effect of this lag is to smooth out over a greater area the abrupt pressure changes which would otherwise occur at the change in surface slope.

The effect of the boundary layer on the pressures on the curved surface of the half-circular-arc airfoil takes a considerably different form from that for a flat plate. At low angles of attack, a strong shock occurs on the curved surface of the airfoil, which is followed by a relatively low Mach number which increases with distance from the leading edge. At the reduced Mach numbers over the forepart of the surface, the rate of growth of the boundary layer is relatively slow. Further back along the surface where the Mach number is higher with a consequently lower density, the boundary layer thickens rapidly. The result of this increase in the rate of boundary-layer growth is an increase in the pressures over the entire curved surface rather than primarily near the leading edge as in the case of the flat plate.

Span-load distribution.— As shown by figure 12, over the upper surface the spanwise variation of the normal-force coefficient is nearly constant but the experimental values of section normal-force coefficient are only about one-half of the values predicted by theory for two-dimensional flow. The data of figure 11 together with figure 4 indicate that the flow is separated just back of the maximum thickness, a condition which is evident at all four spanwise stations. These pressure data show no appreciable effect of the tip over the upper surface even

though at this wing attitude and Mach number the rear 60-percent chord of the outermost spanwise station ($\frac{2y}{b} = 0.904$) of the upper surface would be in a region of three-dimensional flow. Thus, the constancy of the normal force along the span on the upper surface is largely due to separated flow on the entire rear half of the wing.

The results from lower surface pressures (fig. 12) show good agreement with theory in the region of two-dimensional flow but also indicate a gradual decrease in normal force as the tip is approached. The pressure data of figure 11 show that essentially two-dimensional flow exists over the two innermost spanwise stations and that the section normal force in this region of two-dimensional flow is in good agreement with theory. At the two outermost spanwise stations, however, three-dimensional flows exist. Calculations show that three-dimensional flows existed over the rear 10-percent chord at the $\frac{2y}{b} = 0.624$ station and over the rear 80-percent chord at the $\frac{2y}{b} = 0.904$ station.

Base pressures on the wedge airfoil section.— The plots of base pressure against angle of attack in figure 13 indicate that the interference near the midspan ($\frac{2y}{b} = 0.140$) was appreciable for negative angles of attack where the model was supported from the under side. The curves would be symmetrical about zero angle of attack if no interference effects were present. Except for the station nearest the midspan, the spanwise variation of base pressure appeared to be within the scatter of the data. The base pressure varied between $\frac{P_b - P_1}{P_1} = -0.47$ at $\alpha = 0$ to about $\frac{P_b - P_1}{P_1} = -0.55$ at $\alpha = \pm 10^\circ$. A value of $\frac{P_b - P_1}{P_1}$ of -0.50 appears to be representative of the base pressure over the whole range.

Wing Characteristics

Lift.— The agreement in the lift values between the experimental pressure and force data is reasonably good although the values based on force data are slightly below those based on pressure measurements. (See figs. 14, 16, 18, and 20.) This decrement is ascribed to viscous and tip effects. There is no available theoretical method for rigorous calculation of the characteristics of complete wings. However, it may be possible to use the linearized theory to obtain an approximate evaluation of the tip effects. The linearized theory predicts a reduction

of about 7 percent in the lift-curve slope due to tip effect, and an analysis of the pressure data indicates that the section lift-curve slope is reduced by about 12 percent at low angles of attack decreasing to about 4 percent at high angles of attack due to viscous effects. Thus an average total reduction of about 15 percent from the inviscid theory is indicated in the lift-curve slope; however, the force data for the diamond wing are only about 10 percent below the inviscid theory, an indication that the tip effect is overestimated by the linearized theory. In general, the other airfoils show this same effect and the tip effects appear to cause only a 2- to 6-percent reduction in lift. Further investigation is required to evaluate the tip effect more accurately.

At moderate angles of attack, the flow separates at about the maximum thickness on the wing with the diamond section as shown in the schlieren photograph (fig. 24). Similar separations occur on the other wings. At these moderate angles of attack, the lift contribution of the upper surfaces is about 60 percent of the theoretical. At higher angles of attack, the flow separates further forward on the upper surface and decreases the lift slightly. Complete loss of lift on the upper surface, however, does not occur for the wings having the diamond, half-diamond, and circular-arc airfoil sections. The schlieren photograph presented in figure 25 shows that the separation does not occur immediately behind the leading edge. As a result, the pressures on the suction surface remain well below the free-stream pressure. Complete separation from the suction surface was observed for the wing with the wedge airfoil section at an angle of attack of 20° (though complete separation was not noted on the other wings even when the angle of attack of the suction surface was greater than that of wedge airfoil).

Drag.- At very low angles of attack, the drag from the pressure measurements was in good agreement with the values predicted by the nonviscous theory. (See figs. 14, 16, 18, and 20.) The drag from the force measurements at these low angles, however, was appreciably greater than that obtained from the pressure data. This increase in drag is primarily due to skin friction since the pressure effects due to the boundary layer on the various parts of the wings tend to compensate each other. The addition of the calculated friction drag coefficient (see PRESENTATION OF RESULTS) to the results from nonviscous theory resulted in theoretical values which were in good agreement with the experimental values. As the angle of attack was increased, however, the experimental drag coefficients tended toward slightly lower values than predicted by theory because of the loss in lift from the upper surface and tip effects.

Lift-drag ratios.- The lift-drag ratios computed from both force and pressure data agree with the theoretical lift-drag ratios at high

angles of attack (figs. 15, 17, 19, and 21). At low angles of attack, however, the experimental lift-drag ratios obtained from pressure data agree reasonably well with the inviscid theory. The force data agree with the theory including friction, although considerable scatter in the force data is evident at low angles of attack. This scatter is due largely to the forces at the low angles of attack being very small and decreasing the percentage accuracy of the force balance; however, the low-angle force measurements are of sufficient accuracy to indicate that the friction coefficients are of the correct magnitude.

The values of maximum lift-drag ratio obtained from pressure data vary considerably with wing airfoil section but are practically constant when computed from force data. The value of the maximum L/D ratio obtained from pressure data for the wings are summarized in the following table:

Airfoil	Approx. $(L/D)_{\max}$ from pressure data
Diamond (fig. 15)	$10\frac{1}{2}$ at $\alpha = 3^\circ$
Half-diamond (fig. 17)	$8\frac{1}{2}$ at $\alpha = 4\frac{1}{2}^\circ$
Wedge (fig. 19)	10 at $\alpha = 3^\circ$
Half-circular arc (fig. 21)	$7\frac{1}{2}$ at $\alpha = 5\frac{1}{2}^\circ$

Considerable scatter existed in the force data results; however, these results indicated that the maximum L/D ratio was about 6 for all four airfoils.

In figure 19, for the wedge airfoil the theoretical nonviscous lift-drag ratios have been included for base pressures equal to stream pressure, one-half of stream pressure, and zero absolute pressure. A base pressure of 50 percent of stream pressure was indicated in the base-pressure measurements (fig. 13). Good agreement is obtained between the wedge-airfoil force measurements and the theory including skin friction assuming a base pressure of 50 percent of stream pressure.

The maximum lift-drag ratio for the half-circular-arc airfoil was lower than for the other airfoils; however, the angles of attack at which maximum lift-drag ratio occurred were slightly higher than those for the other airfoils so that at angles of attack above those required

for peak L/D the lift-drag ratios were only slightly different. At lower angles of attack, however, considerably lower lift-drag ratios were obtained.

Center of pressure.- In all cases, good agreement was obtained between the experiment and the theory for the centers of pressure (figs. 15, 17, 19, and 21). The locations of the center of pressure on the diamond airfoil sections varied from 40 percent to 45 percent of the chord (fig. 15). The wedge airfoil, as was to be expected, had a center of pressure of 50 percent of the chord over the whole range of angles of attack tested (fig. 19). For the wings with the half-diamond section and the half-circular-arc section the center of pressure moved rapidly away from the midchord position as the angle of zero lift was approached (figs. 17 and 21).

Wing Comparisons

The inviscid theory and the results of pressure measurements indicate that the wing with the diamond and the wedge airfoils are considerably better than those with the half-diamond and the half-circular-arc airfoils when $(L/D)_{\max}$ is considered; however, when viscous effects are included, the difference in $(L/D)_{\max}$ is small and the choice of airfoil would probably be based on other considerations for this Reynolds number. The minimum drag of the wings with the diamond and the wedge airfoils is slightly less than that of the wings having the other two sections but the drag of these two wings increases much more rapidly with angle of attack. Since the minimum drag of the wings is largely composed of skin friction, only moderate percentage reductions in total drag could be obtained by reducing the thickness ratio below 5 percent at the test Reynolds number.

CONCLUSIONS

The results of tests of four wings of square plan form and 5-percent-thick diamond, half-diamond, wedge, and half-circular-arc airfoil sections in the Langley 11-inch hypersonic tunnel at a Mach number of 6.86 and a Reynolds number of 980,000 lead to the following conclusions:

1. Aerodynamic characteristics due to the pressure forces can be predicted with reasonable accuracy by two-dimensional inviscid theory for wings of square plan form at a Mach number of 6.86. At high angles of attack, the experimental results were, however, slightly lower than the value given by the inviscid theory because of separation and tip

effects, and at low angles of attack, the skin friction should be taken into account in calculating the total drag coefficients and lift-drag ratios of wings.

2. The two wings having symmetrical airfoil sections (the diamond and wedge sections) had the highest maximum lift-drag ratios from pressure measurements and the half-circular-arc section had the lowest. The differences, however, were small when viscous effects were included, the over-all maximum lift-drag ratio being close to 6 for all the wings tested.

3. Large deviations of the pressures from those predicted from inviscid theory existed at the leading edge of the wing and just back of sudden changes in surface slope because of a rapid growth of the laminar boundary layer at the high test Mach number.

4. The effect of boundary layer on the pressures on a flat surface parallel to the stream was in good agreement with theoretical results in which the boundary layer was assumed to be laminar.

Langley Aeronautical Laboratory
National Advisory Committee for Aeronautics
Langley Field, Va.

REFERENCES

1. McLellan, Charles H., Williams, Thomas W., and Bertram, Mitchel H.: Investigation of a Two-Step Nozzle in the Langley 11-Inch Hypersonic Tunnel. NACA TN 2171, 1950.
2. McLellan, Charles H., Williams, Thomas W., and Beckwith, Ivan E.: Investigation of the Flow through a Single-Stage Two-Dimensional Nozzle in the Langley 11-Inch Hypersonic Tunnel. NACA TN 2223, 1950.
3. Busemann, A.: Gasströmung mit laminarer Grenzschicht entlang einer Platte. Z.f.a.M.M., Bd. 15, Heft 1/2, Feb. 1935, pp. 23-25.
4. Von Kármán, Th., and Tsien, H. S.: Boundary Layer in Compressible Fluids. Jour. Aero. Sci., vol. 5, no. 6, April 1938, pp. 227-232.

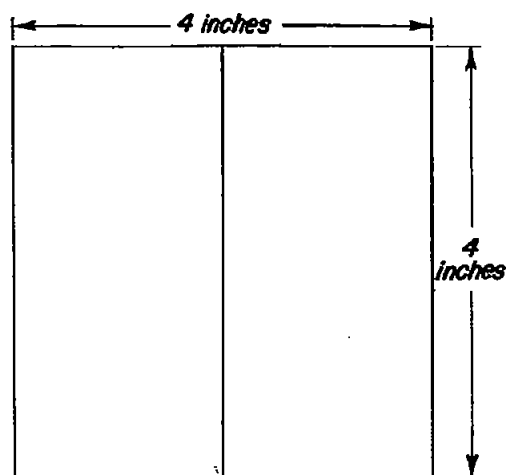
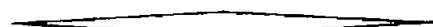
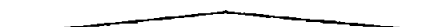
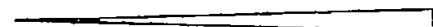
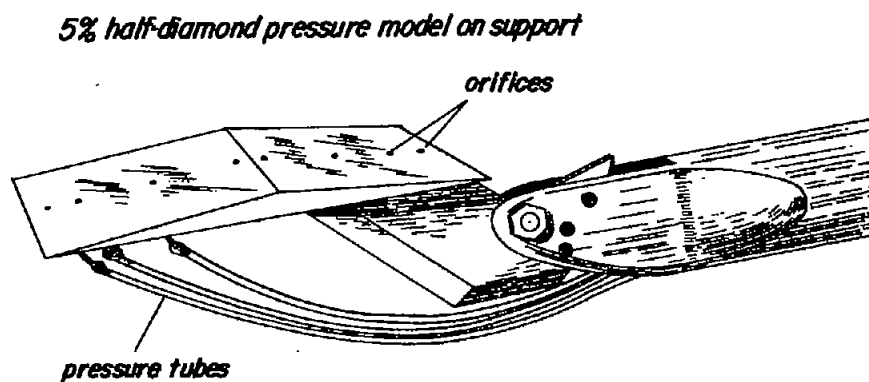
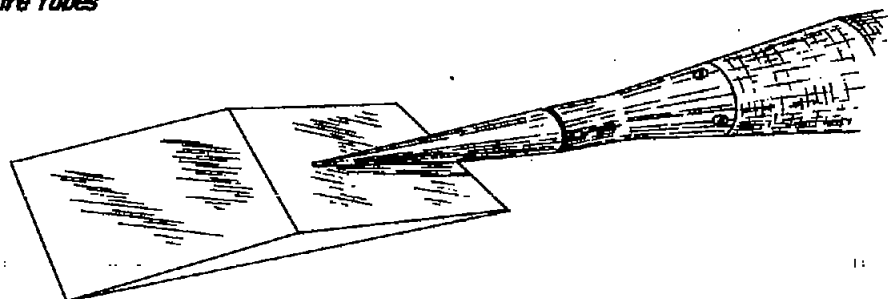
*Plan view**5% diamond**5% half-diamond**5% wedge**5% half-circular arc**5% half-diamond pressure model on support**5% half-diamond force model on support*

Figure 1.- Sketch of the airfoil models used to obtain aerodynamic characteristics at $M = 6.86$.

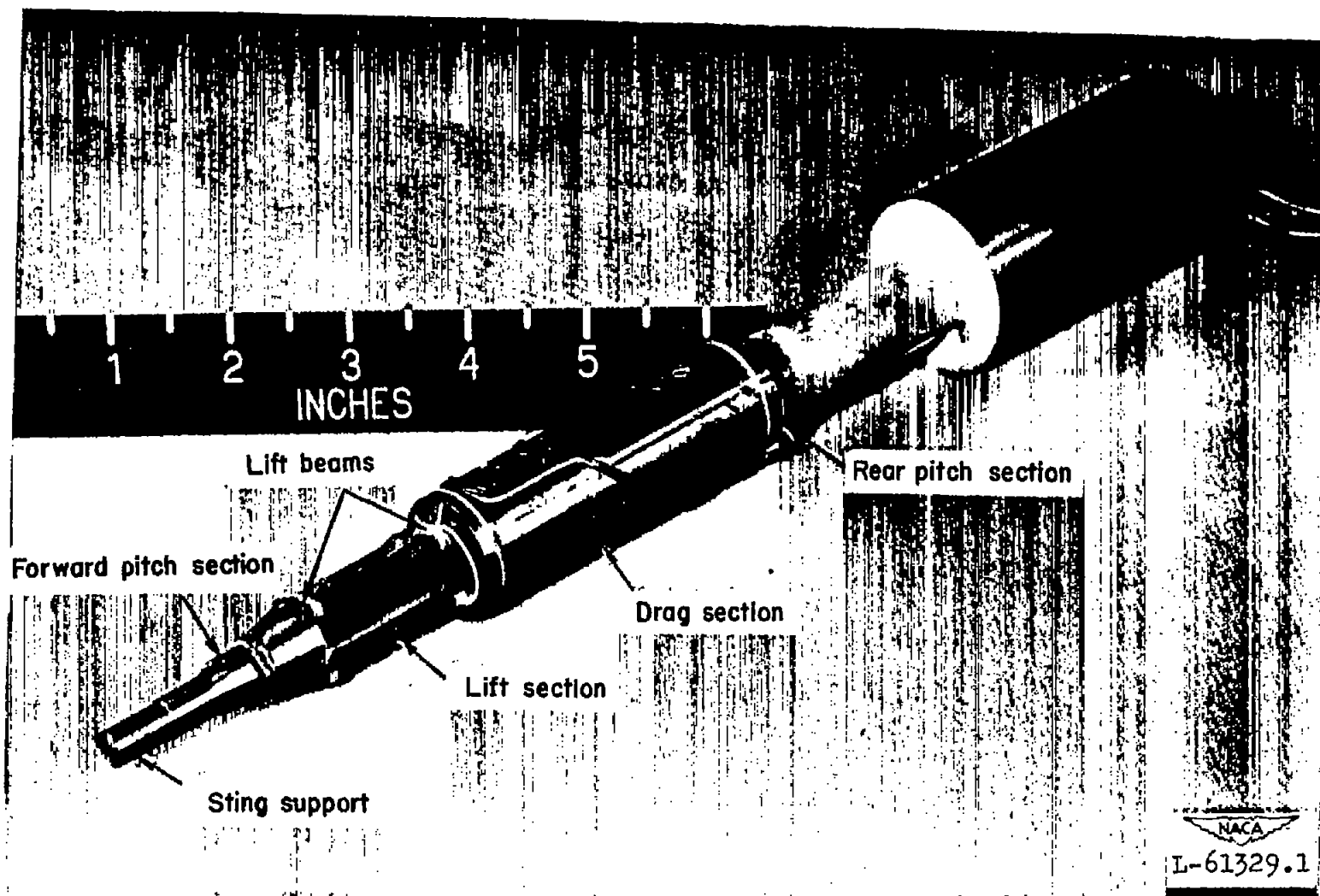


Figure 2.- Views of the disassembled three-component force balance.

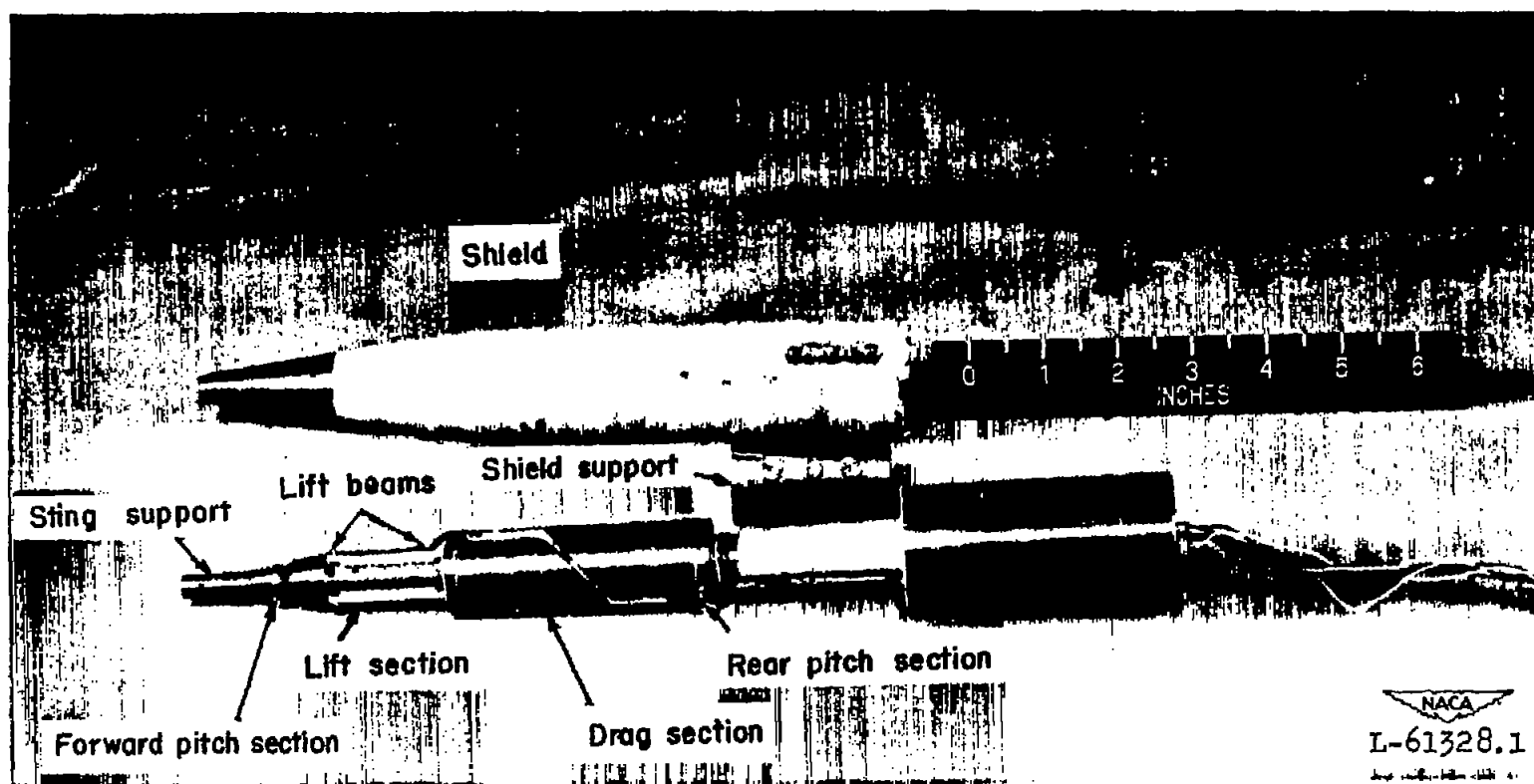


Figure 2.- Concluded.

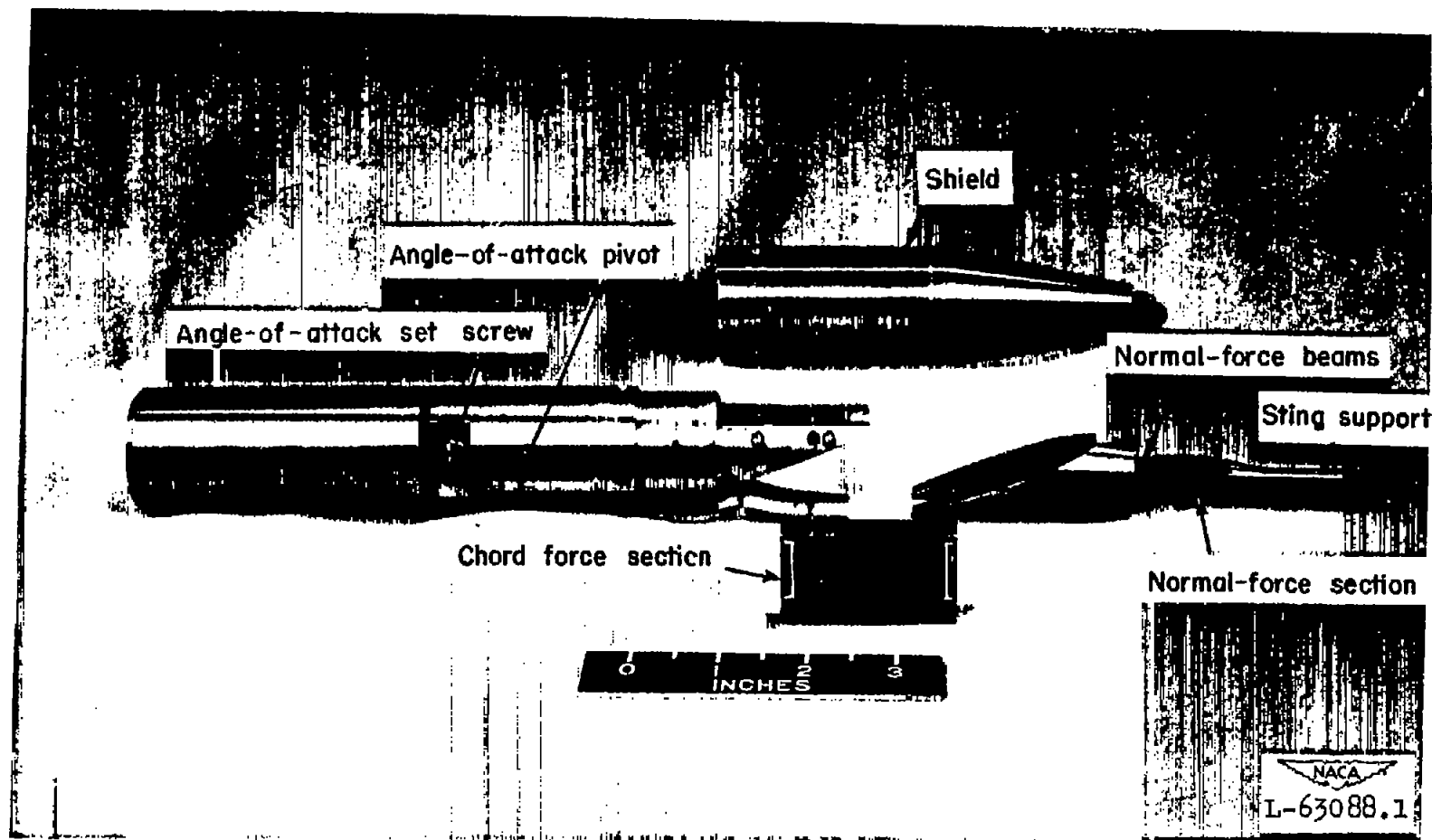
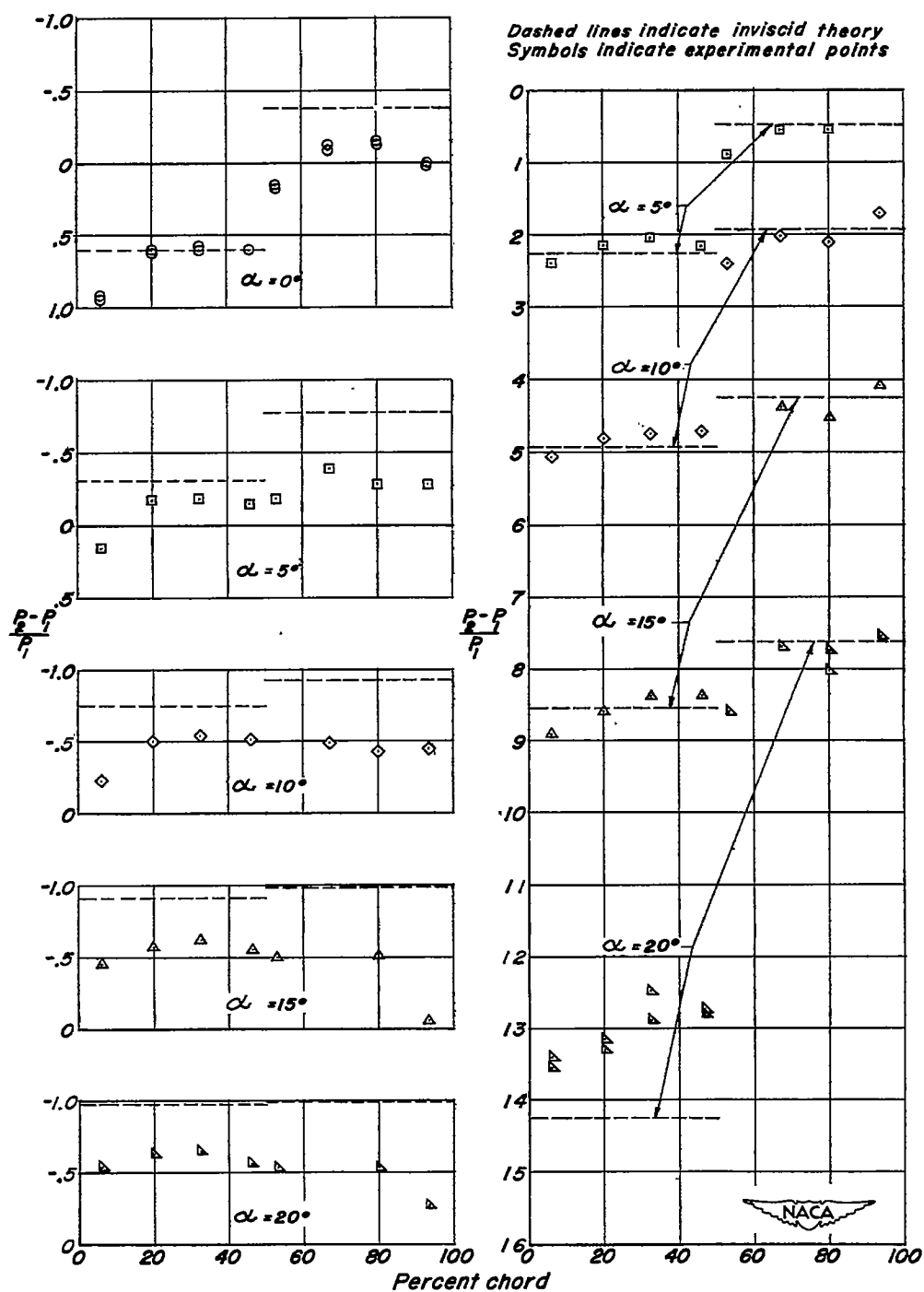


Figure 3.- View of the disassembled two-component sensitive force balance.



(a) Upper surface.

(b) Lower surface.

Figure 4.- The pressure variation over a 5-percent-thick diamond-airfoil section at various angles of attack. $M = 6.86$ and $Re = 0.98 \times 10^6$.

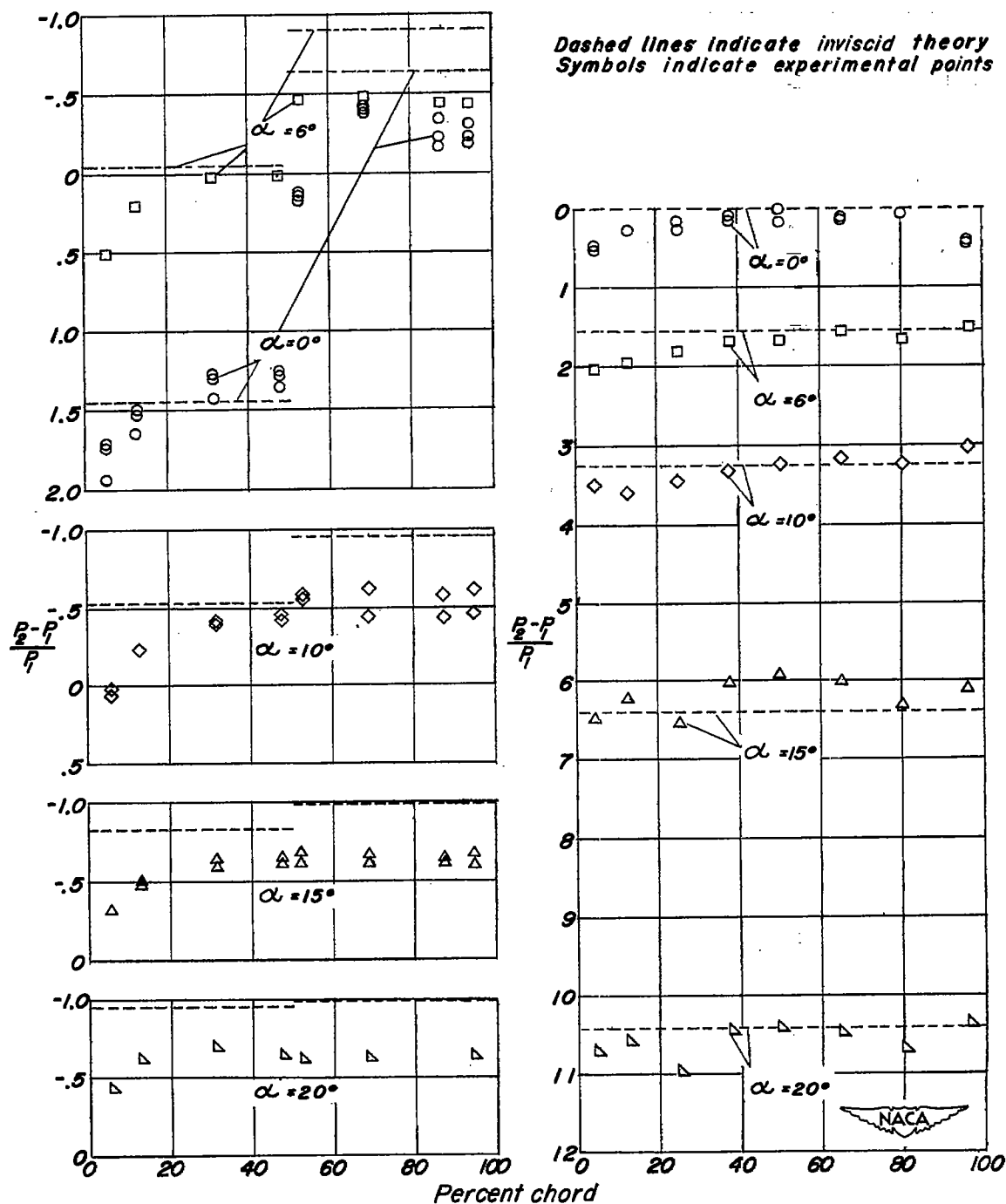


Figure 5.- The pressure variation over a 5-percent-thick half-diamond-airfoil section at various positive angles of attack. $M = 6.86$ and $R = 0.98 \times 10^6$.

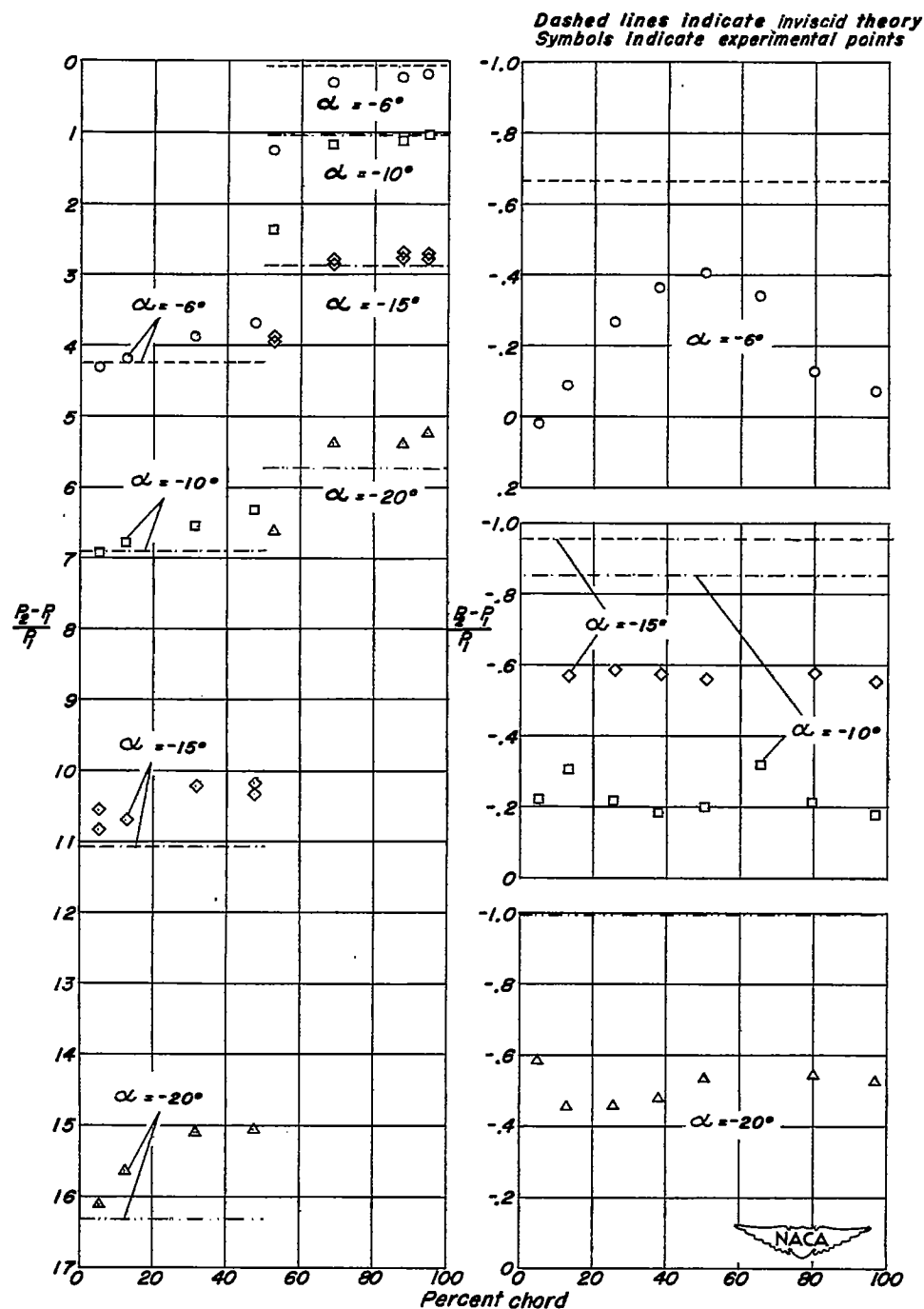


Figure 6.- The pressure variation over a 5-percent-thick half-diamond-airfoil section at various negative angles of attack. $M = 6.86$ and $Re = 0.98 \times 10^6$.

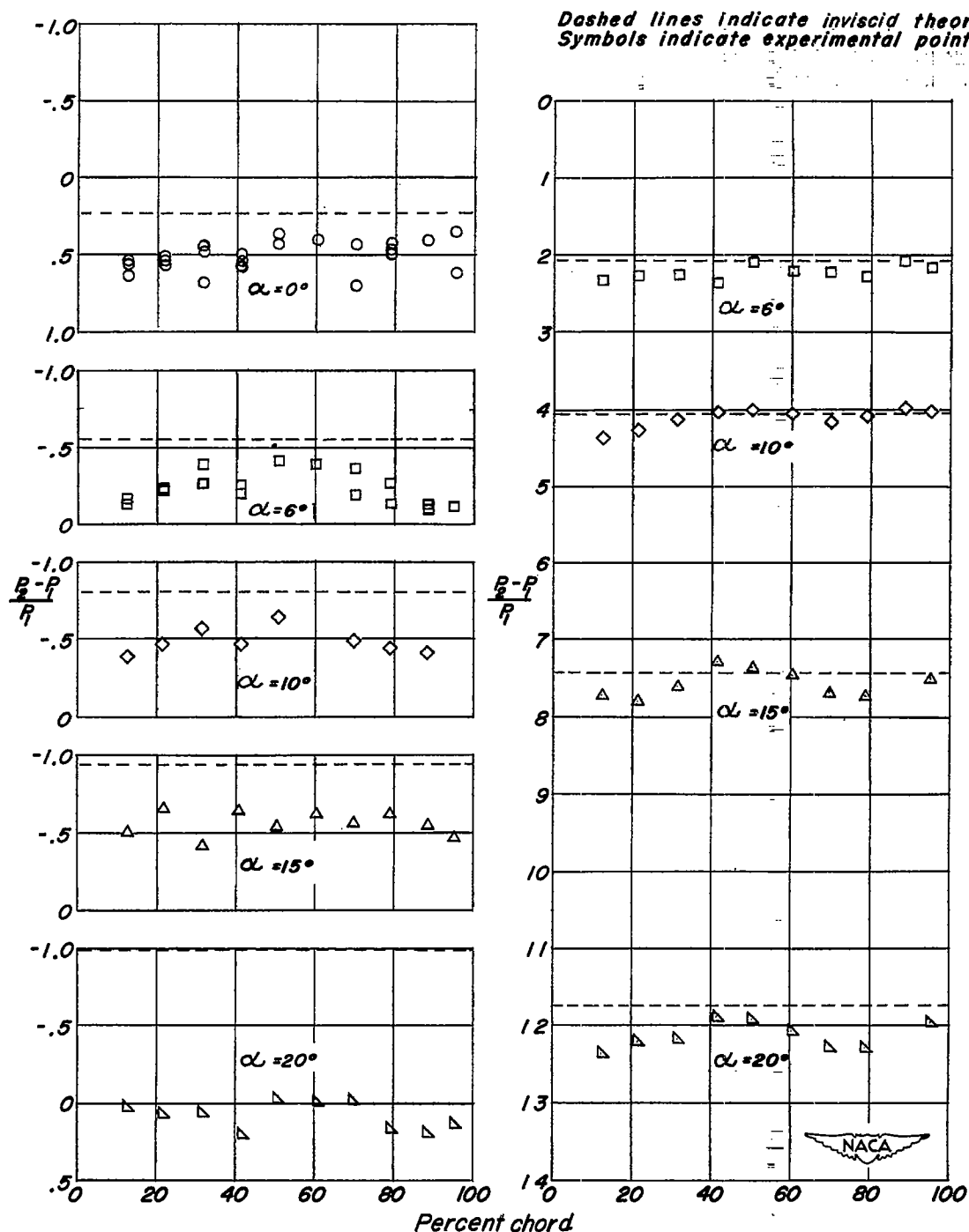


Figure 7.- The pressure variation over a 5-percent-thick wedge-airfoil section at various angles of attack. $M = 6.86$ and $R = 0.98 \times 10^6$.

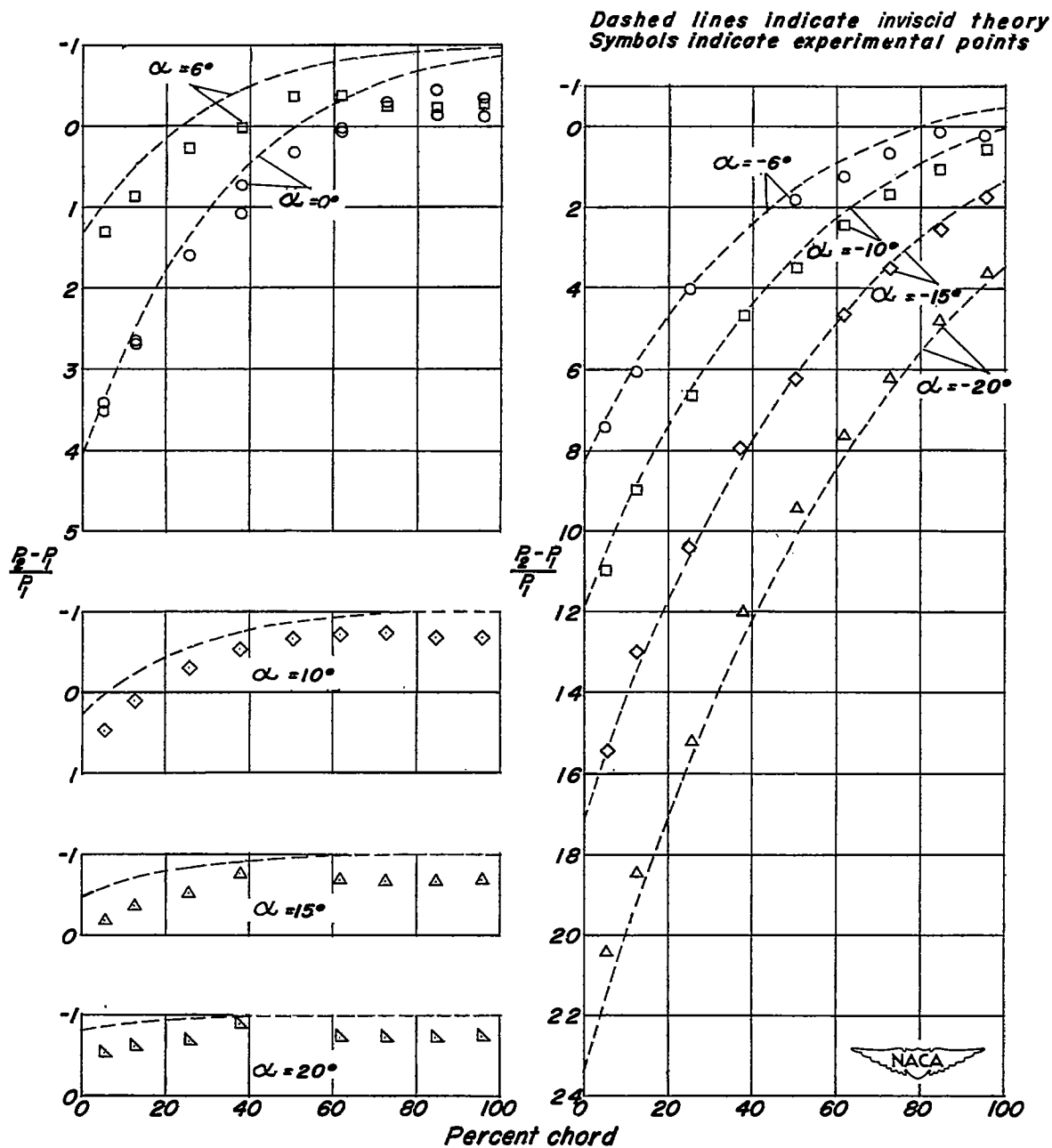
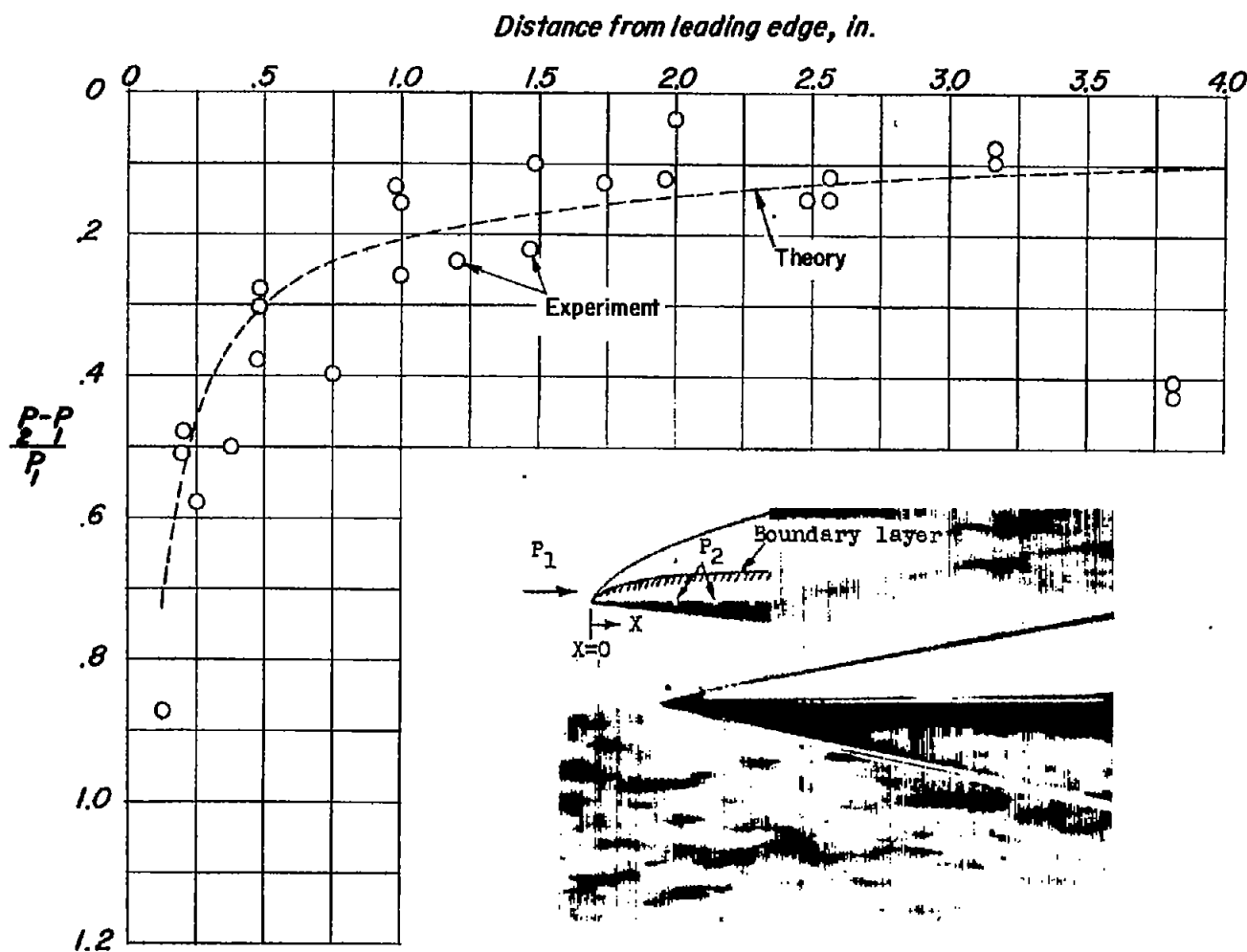


Figure 8.- The pressure variation over the upper surface of a 5-percent-thick half-circular-arc airfoil section at various angles of attack.

$M = 6.86$ and $R = 0.98 \times 10^6$.



NACA
L-69125

Figure 9.- The pressure distribution over a flat plate inclined at zero angle to an initial flow at $M = 6.86$ and $R = 0.98 \times 10^6$.

1	2	3	4	5	6	7	8	9	10	11	12	13	14	15	16	17	18	19	20	21	22	23	24	25	26	27	28	29	30	31	32	33	34	35	36	37	38	39	40	41	42	43	44	45	46	47	48	49	50	51	52	53	54	55	56	57	58	59	60	61	62	63	64	65	66	67	68	69	70	71	72	73	74	75	76	77	78	79	80	81	82	83	84	85	86	87	88	89	90	91	92	93	94	95	96	97	98	99	100	101	102	103	104	105	106	107	108	109	110	111	112	113	114	115	116	117	118	119	120	121	122	123	124	125	126	127	128	129	130	131	132	133	134	135	136	137	138	139	140	141	142	143	144	145	146	147	148	149	150	151	152	153	154	155	156	157	158	159	160	161	162	163	164	165	166	167	168	169	170	171	172	173	174	175	176	177	178	179	180	181	182	183	184	185	186	187	188	189	190	191	192	193	194	195	196	197	198	199	200	201	202	203	204	205	206	207	208	209	210	211	212	213	214	215	216	217	218	219	220	221	222	223	224	225	226	227	228	229	230	231	232	233	234	235	236	237	238	239	240	241	242	243	244	245	246	247	248	249	250	251	252	253	254	255	256	257	258	259	260	261	262	263	264	265	266	267	268	269	270	271	272	273	274	275	276	277	278	279	280	281	282	283	284	285	286	287	288	289	290	291	292	293	294	295	296	297	298	299	300	301	302	303	304	305	306	307	308	309	310	311	312	313	314	315	316	317	318	319	320	321	322	323	324	325	326	327	328	329	330	331	332	333	334	335	336	337	338	339	340	341	342	343	344	345	346	347	348	349	350	351	352	353	354	355	356	357	358	359	360	361	362	363	364	365	366	367	368	369	370	371	372	373	374	375	376	377	378	379	380	381	382	383	384	385	386	387	388	389	390	391	392	393	394	395	396	397	398	399	400	401	402	403	404	405	406	407	408	409	410	411	412	413	414	415	416	417	418	419	420	421	422	423	424	425	426	427	428	429	430	431	432	433	434	435	436	437	438	439	440	441	442	443	444	445	446	447	448	449	450	451	452	453	454	455	456	457	458	459	460	461	462	463	464	465	466	467	468	469	470	471	472	473	474	475	476	477	478	479	480	481	482	483	484	485	486	487	488	489	490	491	492	493	494	495	496	497	498	499	500	501	502	503	504	505	506	507	508	509	510	511	512	513	514	515	516	517	518	519	520	521	522	523	524	525	526	527	528	529	530	531	532	533	534	535	536	537	538	539	540	541	542	543	544	545	546	547	548	549	550	551	552	553	554	555	556	557	558	559	560	561	562	563	564	565	566	567	568	569	570	571	572	573	574	575	576	577	578	579	580	581	582	583	584	585	586	587	588	589	590	591	592	593	594	595	596	597	598	599	600	601	602	603	604	605	606	607	608	609	610	611	612	613	614	615	616	617	618	619	620	621	622	623	624	625	626	627	628	629	630	631	632	633	634	635	636	637	638	639	640	641	642	643	644	645	646	647	648	649	650	651	652	653	654	655	656	657	658	659	660	661	662	663	664	665	666	667	668	669	670	671	672	673	674	675	676	677	678	679	680	681	682	683	684	685	686	687	688	689	690	691	692	693	694	695	696	697	698	699	700	701	702	703	704	705	706	707	708	709	710	711	712	713	714	715	716	717	718	719	720	721	722	723	724	725	726	727	728	729	730	731	732	733	734	735	736	737	738	739	740	741	742	743	744	745	746	747	748	749	750	751	752	753	754	755	756	757	758	759	760	761	762	763	764	765	766	767	768	769	770	771	772	773	774	775	776	777	778	779	780	781	782	783	784	785	786	787	788	789	790	791	792	793	794	795	796	797	798	799	800	801	802	803	804	805	806	807	808	809	810	811	812	813	814	815	816	817	818	819	820	821	822	823	824	825	826	827	828	829	830	831	832	833	834	835	836	837	838	839	840	841	842	843	844	845	846	847	848	849	850	851	852	853	854	855	856	857	858	859	860	861	862	863	864	865	866	867	868	869	870	871	872	873	874	875	876	877	878	879	880	881	882	883	884	885	886	887	888	889	890	891	892	893	894	895	896	897	898	899	900	901	902	903	904	905	906	907	908	909	910	911	912	913	914	915	916	917	918	919	920	921	922	923	924	925	926	927	928	929	930	931	932	933	934	935	936	937	938	939	940	941	942	943	944	945	946	947	948	949	950	951	952	953	954	955	956	957	958	959	960	961	962	963	964	965	966	967	968	969	970	971	972	973	974	975	976	977	978	979	980	981	982	983	984	985	986	987	988	989	990	991	992	993	994	995	996	997	998	999	1000	1001	1002	1003	1004	1005	1006	1007	1008	1009	1010	1011	1012	1013	1014	1015	1016	1017	1018	1019	1020	1021	1022	1023	1024	1025	1026	1027	1028	1029	1030	1031	1032	1033	1034	1035	1036	1037	1038	1039	1040	1041	1042	1043	1044	1045	1046	1047	1048	1049	1050	1051	1052	1053	1054	1055	1056	1057	1058	1059	1060	1061	1062	1063	1064	1065	1066	1067	1068	1069	1070	1071	1072	1073	1074	1075	1076	1077	1078	1079	1080	1081	1082	1083	1084	1085	1086	1087	1088	1089	1090	1091	1092	1093	1094	1095	1096	1097	1098	1099	1100	1101	1102	1103	1104	1105	1106	1107	1108	1109	1110	1111	1112	1113	1114	1115	1116	1117	1118	1119	1120	1121	1122	1123	1124	1125	1126	1127	1128	1129	1130	1131	1132	1133	1134	1135	1136	1137	1138	1139	1140	1141	1142	1143	1144	1145	1146	1147	1148	1149	1150	1151	1152	1153	1154	1155	1156	1157	1158	1159	1160	1161	1162	1163	1164	1165	1166	1167	1168	1169	1170	1171	1172	1173	1174	1175	1176	1177	1178	1179	1180	1181	1182	1183	1184	1185	1186	1187	1188	1189	1190	1191	1192	1193	1194	1195	1196	1197	1198	1199	1200	1201	1202	1203	1204	1205	1206	1207	1208	1209	1210	1211	1212	1213	1214	1215	1216	1217	1218	1219	1220	1221	1222	1223	1224	1225	1226	1227	1228	1229	1230	1231	1232	1233	1234	1235	1236	1237	1238	1239	1240	1241	1242	1243	1244	1245	1246	1247	1248	1249	1250	1251	1252	1253	1254	1255	1256	1257	1258	1259	1260	1261	1262	1263	1264	1265	1266	1267	1268	1269	1270	1271	1272	1273	1274	1275	1276	1277	1278	1279	1280	1281	1282	1283	1284	1285	1286	1287	1288	1289	1290	1291	1292	1293	1294	1295	1296	1297	1298	1299	1300	1301	1302	1303	1304	1305	1306	1307	1308	1309	1310	1311	1312	1313	1314	1315	1316	1317	1318	1319	1320	1321	1322	1323	1324	1325	1326	1327	1328	1329	1330	1331	1332	1333	1334	1335	1336	1337	1338	1339	1340	1341	1342	1343	1344	1345	1346	1347	1348	1349	1350	1351	1352	1353	1354	1355	1356	1357	1358	1359	1360	1361	1362	1363	1364	1365	1366	1367	1368	1369	1370	1371	1372	1373	1374	1375	1376	1377	1378	1379	1380	1381	1382	1383	1384	1385	1386	1387	1388	1389	1390	1391	1392	1393	1394	1395	1396	1397	1398	1399	1400	1401	1402	1403	1404	1405	1406	1407	1408	1409	1410	1411	1412	1413	1414	1415	1416	1417	1418	1419	1420	1421	1422	1423	1424	1425	1426	1427	1428	1429	1430	1431	1432	1433	1434	1435	1436	1437	1438	1439	1440	1441	1442	1443	1444	1445	1446	1447	1448	1449	1450	1451	1452	1453	1454	1455	1456	1457	1458	1459	1460	1461	1462	1463	1464	1465	1466	1467	1468	1469	1470	1471	1472	1473	1474	1475	1476	1477	1478	1479	1480	1481	1482	1483	1484	1485	1486	1487	1488	1489	1490	1491	1
---	---	---	---	---	---	---	---	---	----	----	----	----	----	----	----	----	----	----	----	----	----	----	----	----	----	----	----	----	----	----	----	----	----	----	----	----	----	----	----	----	----	----	----	----	----	----	----	----	----	----	----	----	----	----	----	----	----	----	----	----	----	----	----	----	----	----	----	----	----	----	----	----	----	----	----	----	----	----	----	----	----	----	----	----	----	----	----	----	----	----	----	----	----	----	----	----	----	----	-----	-----	-----	-----	-----	-----	-----	-----	-----	-----	-----	-----	-----	-----	-----	-----	-----	-----	-----	-----	-----	-----	-----	-----	-----	-----	-----	-----	-----	-----	-----	-----	-----	-----	-----	-----	-----	-----	-----	-----	-----	-----	-----	-----	-----	-----	-----	-----	-----	-----	-----	-----	-----	-----	-----	-----	-----	-----	-----	-----	-----	-----	-----	-----	-----	-----	-----	-----	-----	-----	-----	-----	-----	-----	-----	-----	-----	-----	-----	-----	-----	-----	-----	-----	-----	-----	-----	-----	-----	-----	-----	-----	-----	-----	-----	-----	-----	-----	-----	-----	-----	-----	-----	-----	-----	-----	-----	-----	-----	-----	-----	-----	-----	-----	-----	-----	-----	-----	-----	-----	-----	-----	-----	-----	-----	-----	-----	-----	-----	-----	-----	-----	-----	-----	-----	-----	-----	-----	-----	-----	-----	-----	-----	-----	-----	-----	-----	-----	-----	-----	-----	-----	-----	-----	-----	-----	-----	-----	-----	-----	-----	-----	-----	-----	-----	-----	-----	-----	-----	-----	-----	-----	-----	-----	-----	-----	-----	-----	-----	-----	-----	-----	-----	-----	-----	-----	-----	-----	-----	-----	-----	-----	-----	-----	-----	-----	-----	-----	-----	-----	-----	-----	-----	-----	-----	-----	-----	-----	-----	-----	-----	-----	-----	-----	-----	-----	-----	-----	-----	-----	-----	-----	-----	-----	-----	-----	-----	-----	-----	-----	-----	-----	-----	-----	-----	-----	-----	-----	-----	-----	-----	-----	-----	-----	-----	-----	-----	-----	-----	-----	-----	-----	-----	-----	-----	-----	-----	-----	-----	-----	-----	-----	-----	-----	-----	-----	-----	-----	-----	-----	-----	-----	-----	-----	-----	-----	-----	-----	-----	-----	-----	-----	-----	-----	-----	-----	-----	-----	-----	-----	-----	-----	-----	-----	-----	-----	-----	-----	-----	-----	-----	-----	-----	-----	-----	-----	-----	-----	-----	-----	-----	-----	-----	-----	-----	-----	-----	-----	-----	-----	-----	-----	-----	-----	-----	-----	-----	-----	-----	-----	-----	-----	-----	-----	-----	-----	-----	-----	-----	-----	-----	-----	-----	-----	-----	-----	-----	-----	-----	-----	-----	-----	-----	-----	-----	-----	-----	-----	-----	-----	-----	-----	-----	-----	-----	-----	-----	-----	-----	-----	-----	-----	-----	-----	-----	-----	-----	-----	-----	-----	-----	-----	-----	-----	-----	-----	-----	-----	-----	-----	-----	-----	-----	-----	-----	-----	-----	-----	-----	-----	-----	-----	-----	-----	-----	-----	-----	-----	-----	-----	-----	-----	-----	-----	-----	-----	-----	-----	-----	-----	-----	-----	-----	-----	-----	-----	-----	-----	-----	-----	-----	-----	-----	-----	-----	-----	-----	-----	-----	-----	-----	-----	-----	-----	-----	-----	-----	-----	-----	-----	-----	-----	-----	-----	-----	-----	-----	-----	-----	-----	-----	-----	-----	-----	-----	-----	-----	-----	-----	-----	-----	-----	-----	-----	-----	-----	-----	-----	-----	-----	-----	-----	-----	-----	-----	-----	-----	-----	-----	-----	-----	-----	-----	-----	-----	-----	-----	-----	-----	-----	-----	-----	-----	-----	-----	-----	-----	-----	-----	-----	-----	-----	-----	-----	-----	-----	-----	-----	-----	-----	-----	-----	-----	-----	-----	-----	-----	-----	-----	-----	-----	-----	-----	-----	-----	-----	-----	-----	-----	-----	-----	-----	-----	-----	-----	-----	-----	-----	-----	-----	-----	-----	-----	-----	-----	-----	-----	-----	-----	-----	-----	-----	-----	-----	-----	-----	-----	-----	-----	-----	-----	-----	-----	-----	-----	-----	-----	-----	-----	-----	-----	-----	-----	-----	-----	-----	-----	-----	-----	-----	-----	-----	-----	-----	-----	-----	-----	-----	-----	-----	-----	-----	-----	-----	-----	-----	-----	-----	-----	-----	-----	-----	-----	-----	-----	-----	-----	-----	-----	-----	-----	-----	-----	-----	-----	-----	-----	-----	-----	-----	-----	-----	-----	-----	-----	-----	-----	-----	-----	-----	-----	-----	-----	-----	-----	-----	-----	-----	-----	-----	-----	-----	-----	-----	-----	-----	-----	-----	-----	-----	-----	-----	-----	-----	-----	-----	-----	-----	-----	-----	-----	-----	-----	-----	-----	-----	-----	-----	-----	-----	-----	-----	-----	-----	-----	-----	-----	-----	-----	-----	-----	-----	-----	-----	-----	-----	-----	-----	-----	-----	-----	-----	-----	-----	-----	-----	-----	-----	-----	-----	-----	-----	-----	-----	-----	-----	-----	-----	-----	-----	-----	-----	-----	-----	-----	-----	-----	-----	-----	-----	-----	-----	-----	-----	-----	-----	-----	-----	-----	-----	-----	-----	-----	-----	-----	-----	-----	-----	-----	-----	-----	-----	-----	-----	-----	-----	-----	-----	-----	-----	-----	-----	-----	-----	-----	-----	-----	-----	-----	-----	-----	-----	-----	-----	-----	-----	-----	-----	-----	-----	-----	-----	-----	-----	-----	-----	-----	-----	-----	-----	-----	-----	-----	-----	-----	-----	-----	-----	-----	-----	-----	-----	-----	-----	-----	-----	-----	-----	-----	-----	-----	-----	-----	-----	-----	-----	-----	-----	-----	-----	-----	-----	-----	-----	-----	-----	-----	-----	-----	-----	-----	-----	-----	-----	-----	-----	-----	-----	-----	-----	-----	-----	-----	-----	-----	-----	-----	-----	-----	-----	-----	-----	-----	-----	-----	-----	-----	-----	-----	-----	-----	-----	-----	-----	-----	-----	-----	-----	-----	-----	-----	-----	-----	-----	-----	-----	-----	-----	-----	-----	-----	-----	-----	-----	-----	-----	-----	-----	-----	-----	-----	-----	-----	-----	-----	-----	-----	-----	-----	-----	------	------	------	------	------	------	------	------	------	------	------	------	------	------	------	------	------	------	------	------	------	------	------	------	------	------	------	------	------	------	------	------	------	------	------	------	------	------	------	------	------	------	------	------	------	------	------	------	------	------	------	------	------	------	------	------	------	------	------	------	------	------	------	------	------	------	------	------	------	------	------	------	------	------	------	------	------	------	------	------	------	------	------	------	------	------	------	------	------	------	------	------	------	------	------	------	------	------	------	------	------	------	------	------	------	------	------	------	------	------	------	------	------	------	------	------	------	------	------	------	------	------	------	------	------	------	------	------	------	------	------	------	------	------	------	------	------	------	------	------	------	------	------	------	------	------	------	------	------	------	------	------	------	------	------	------	------	------	------	------	------	------	------	------	------	------	------	------	------	------	------	------	------	------	------	------	------	------	------	------	------	------	------	------	------	------	------	------	------	------	------	------	------	------	------	------	------	------	------	------	------	------	------	------	------	------	------	------	------	------	------	------	------	------	------	------	------	------	------	------	------	------	------	------	------	------	------	------	------	------	------	------	------	------	------	------	------	------	------	------	------	------	------	------	------	------	------	------	------	------	------	------	------	------	------	------	------	------	------	------	------	------	------	------	------	------	------	------	------	------	------	------	------	------	------	------	------	------	------	------	------	------	------	------	------	------	------	------	------	------	------	------	------	------	------	------	------	------	------	------	------	------	------	------	------	------	------	------	------	------	------	------	------	------	------	------	------	------	------	------	------	------	------	------	------	------	------	------	------	------	------	------	------	------	------	------	------	------	------	------	------	------	------	------	------	------	------	------	------	------	------	------	------	------	------	------	------	------	------	------	------	------	------	------	------	------	------	------	------	------	------	------	------	------	------	------	------	------	------	------	------	------	------	------	------	------	------	------	------	------	------	------	------	------	------	------	------	------	------	------	------	------	------	------	------	------	------	------	------	------	------	------	------	------	------	------	------	------	------	------	------	------	------	------	------	------	------	------	------	------	------	------	------	------	------	------	------	------	------	------	------	------	------	------	------	------	------	------	------	------	------	------	------	------	------	------	------	------	------	------	------	------	------	------	------	------	------	------	------	------	------	------	------	------	------	------	------	------	------	------	------	------	------	------	------	------	------	------	------	------	------	------	---

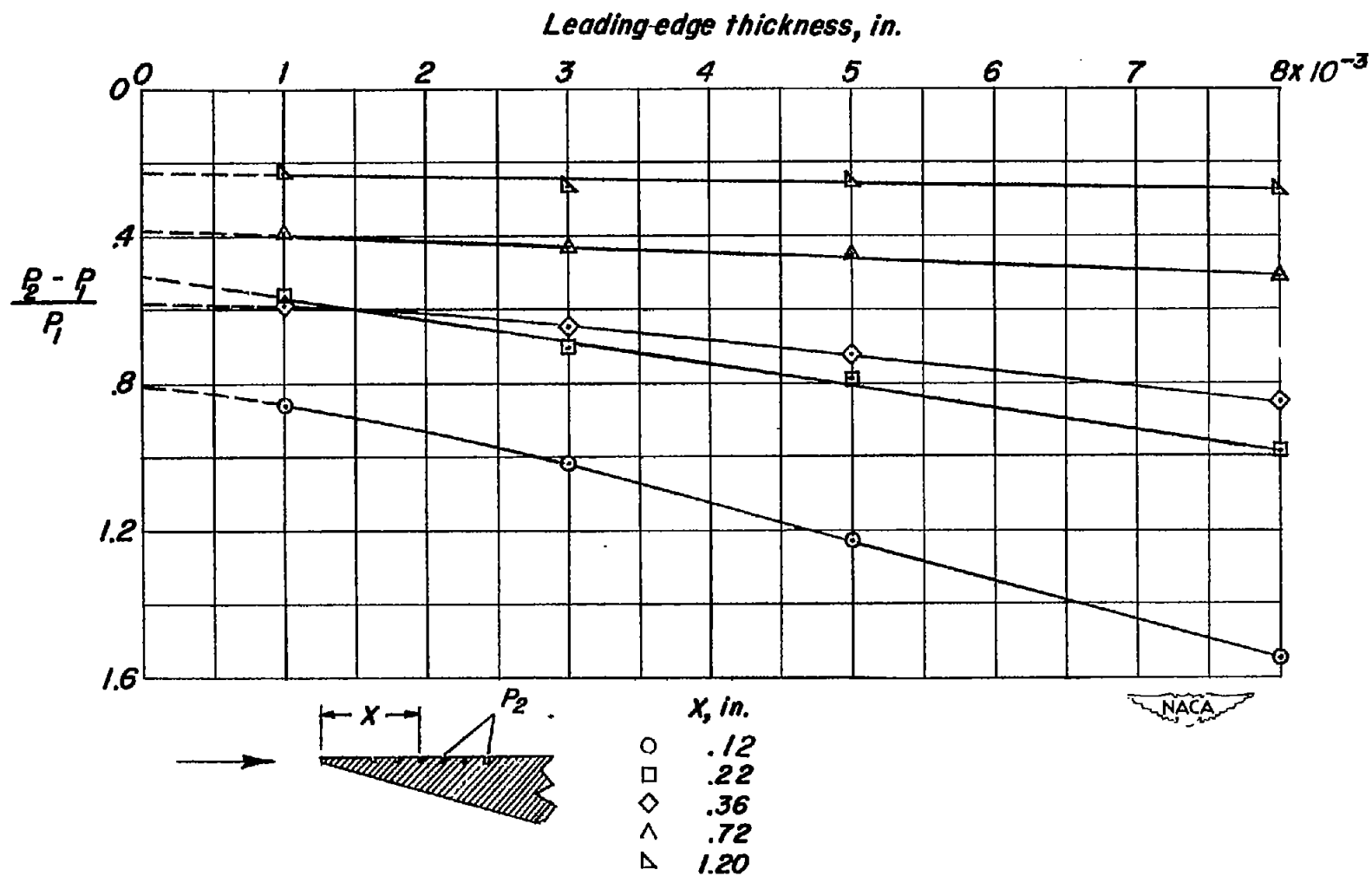


Figure 10.- The effect of leading-edge thickness upon the pressures over a flat plate at zero angle of incidence to flow at $M = 6.86$ and $R = 0.98 \times 10^6$.

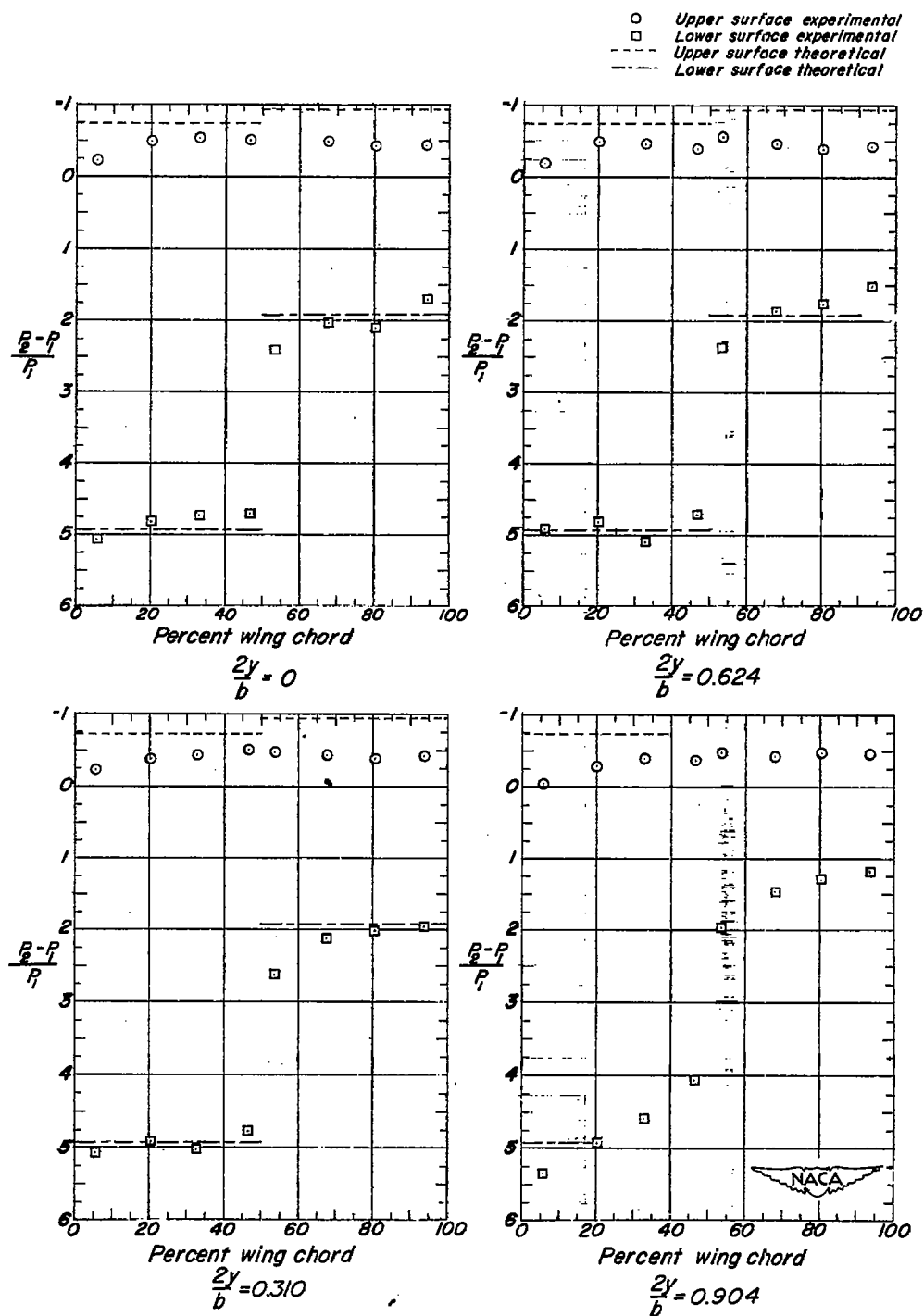


Figure 11.- The chordwise pressure distribution over a 5-percent-thick diamond-section airfoil at $\alpha = 10^\circ$ for various spanwise stations, measured from midspan; $M = 6.86$ and $R = 0.98 \times 10^6$.

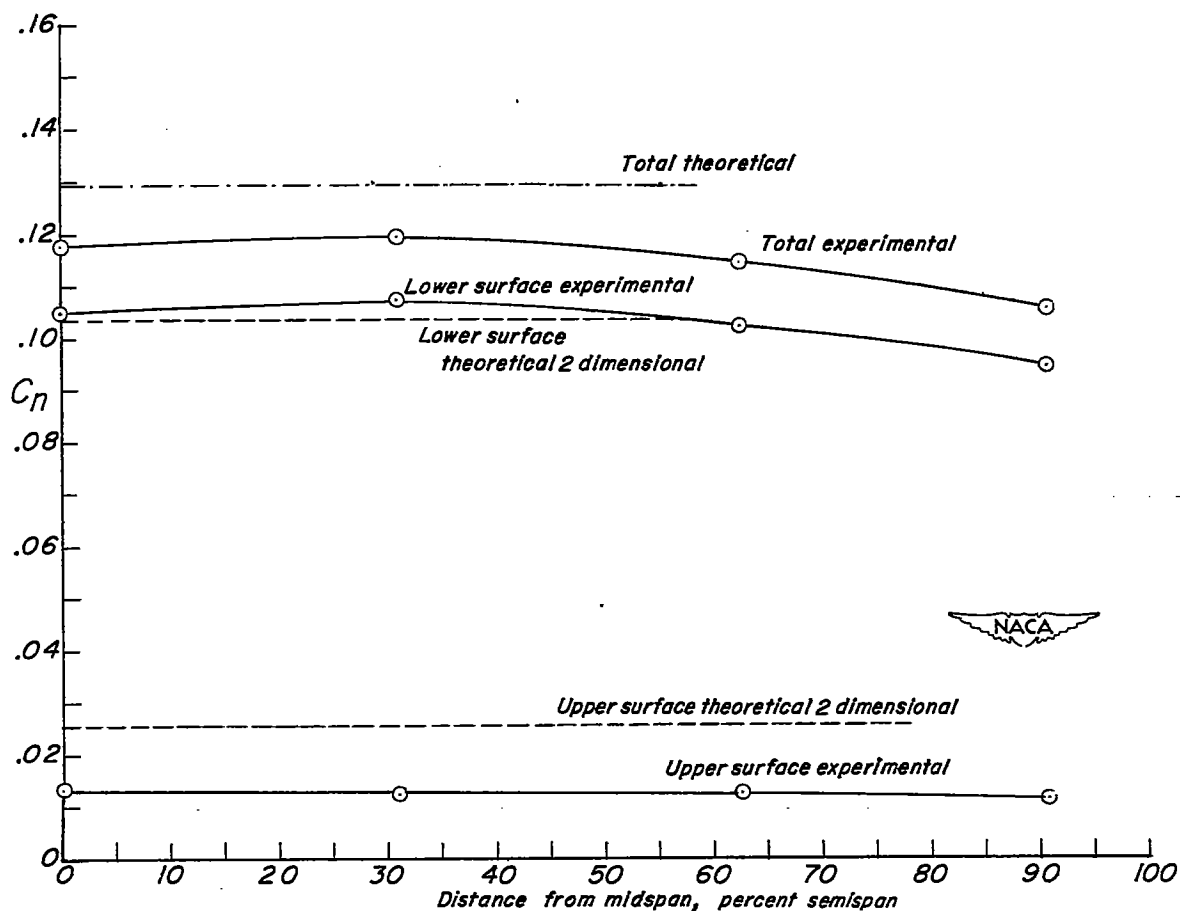


Figure 12.- The spanwise variation of the section normal-force coefficient over the 5-percent-thick diamond airfoil at an angle of attack of 10° .
 $M = 6.86$ and $R = 0.98 \times 10^6$.

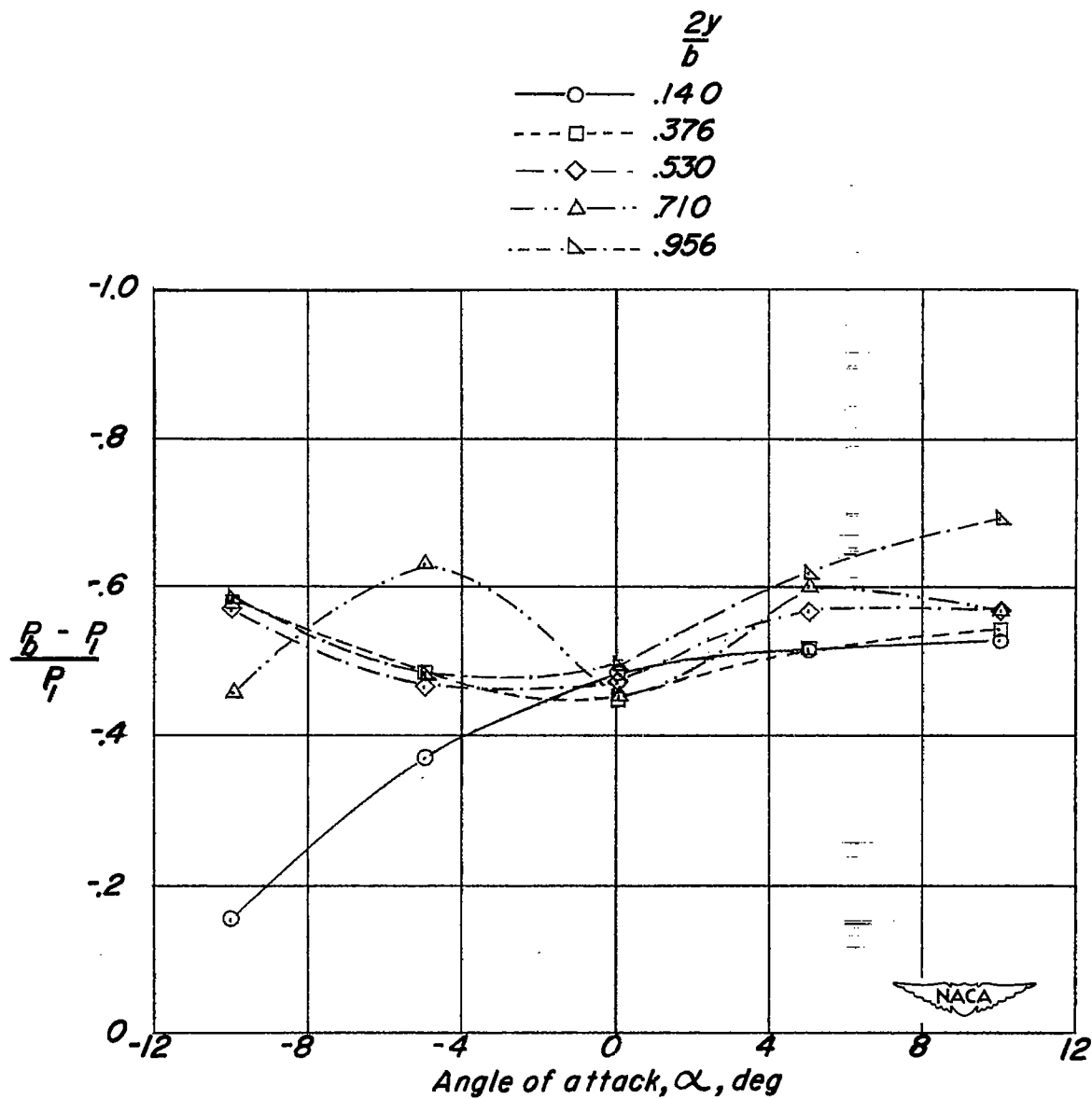


Figure 13.- The base pressures over the wedge airfoil pressure model as a function of angle of attack for various distances from midspan.

$M = 6.86$ and $R = 0.98 \times 10^6$.

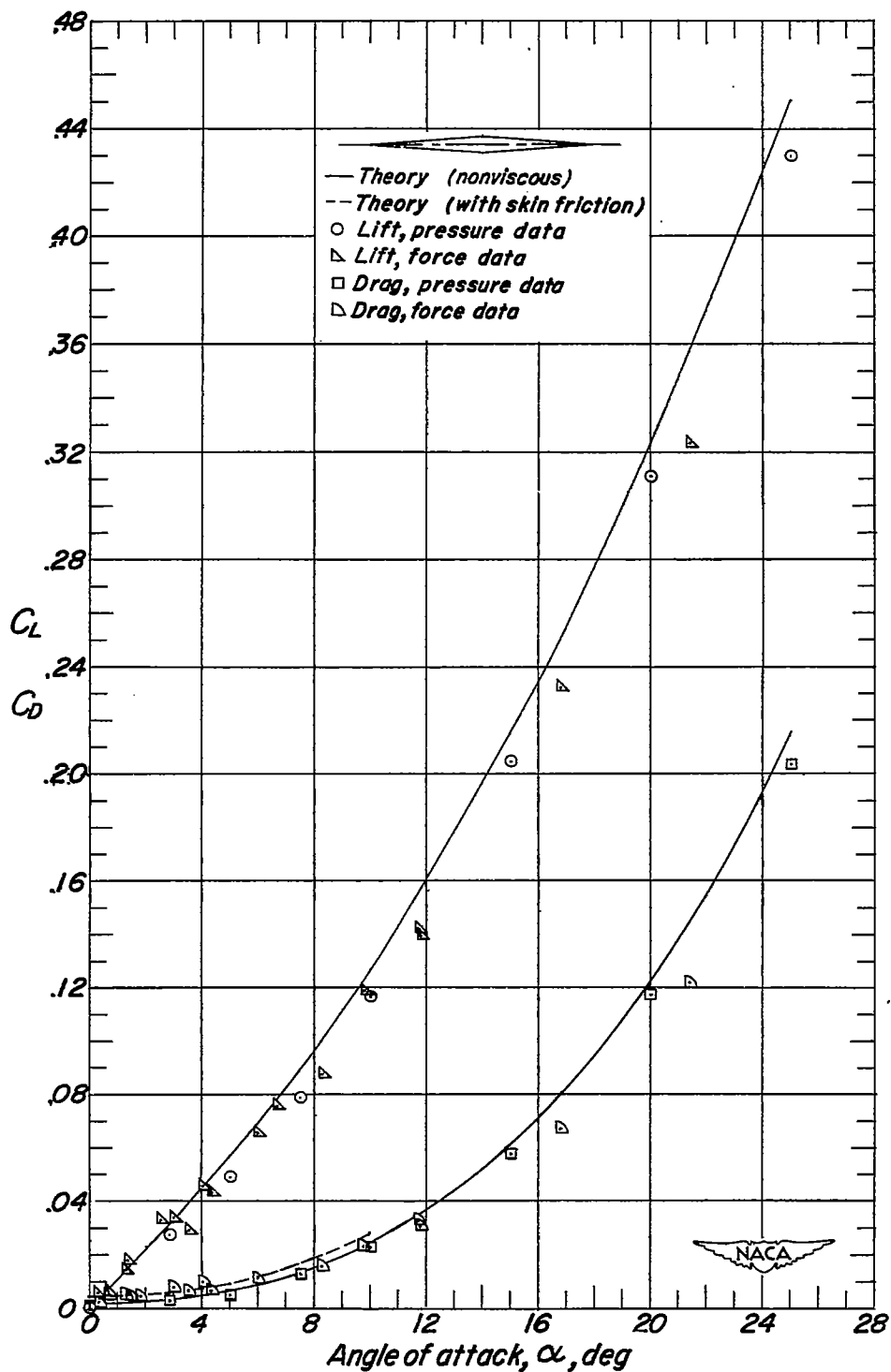


Figure 14.- The variation of the lift and drag coefficients with angle of attack for a 5-percent-thick diamond-section airfoil at $M = 6.86$ and $R = 0.98 \times 10^6$.

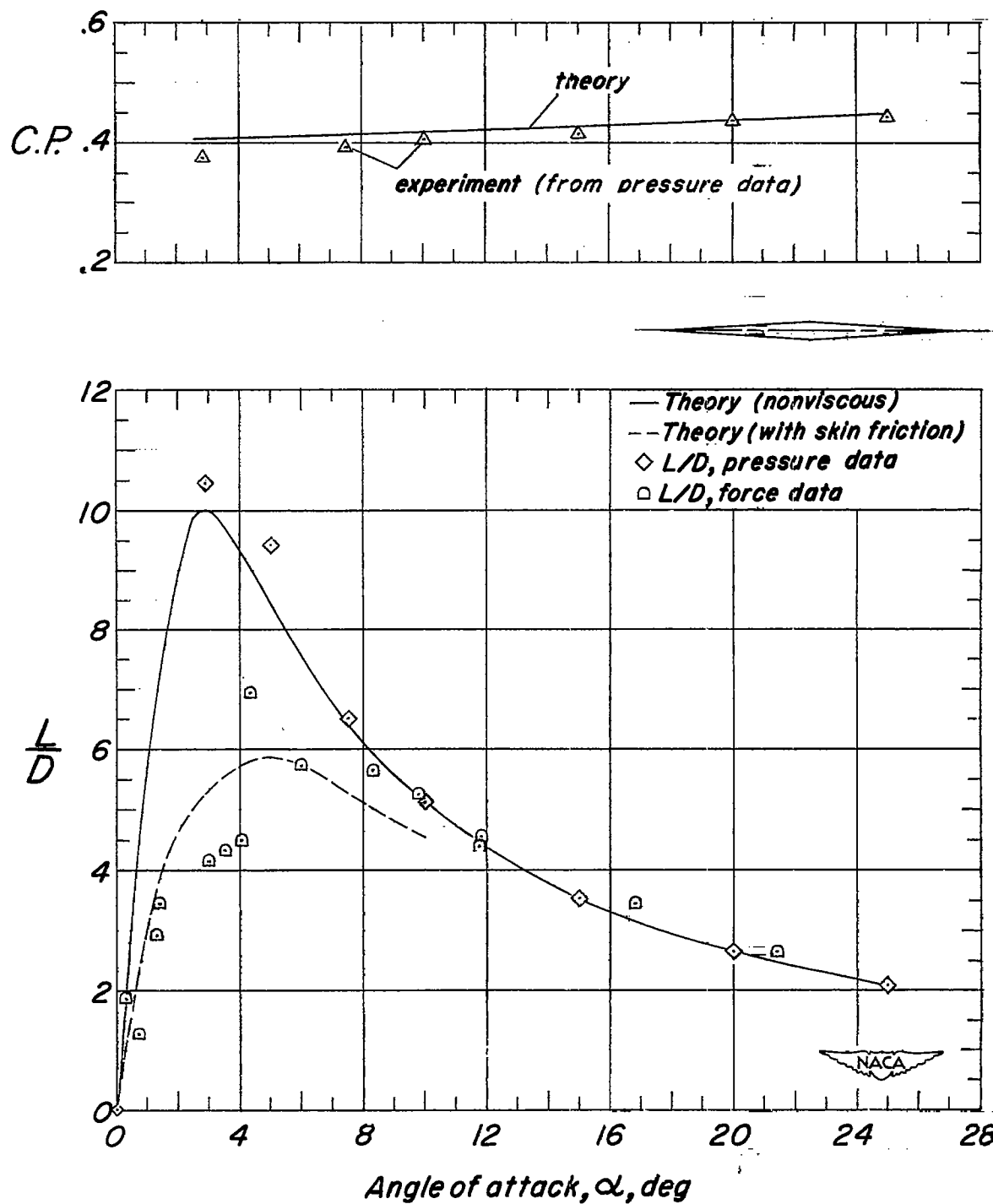


Figure 15.- The variation of the center of pressure and the lift-to-drag ratio with angle of attack for a 5-percent-thick diamond-section airfoil at $M = 6.86$ and $R = 0.98 \times 10^6$.

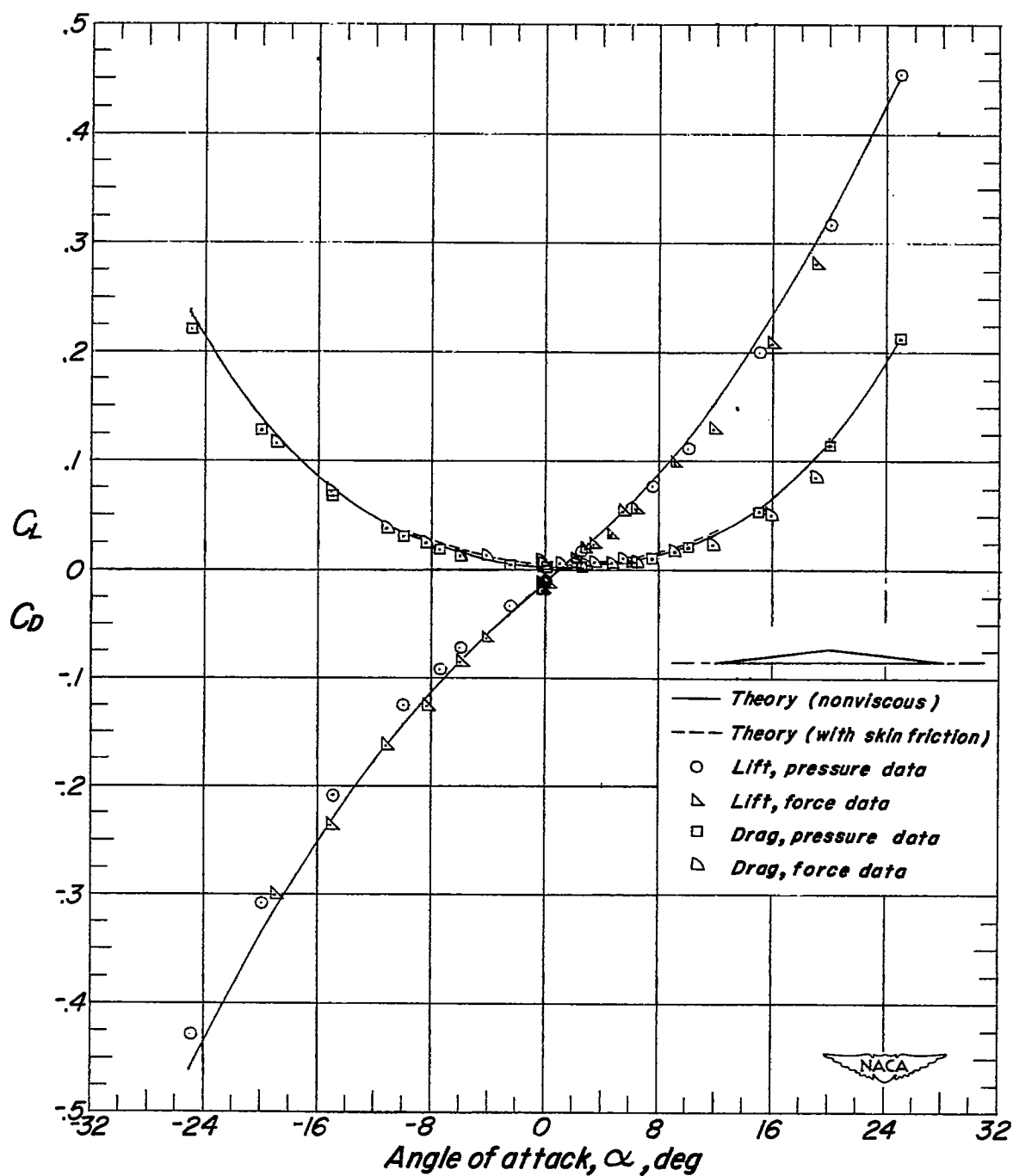


Figure 16.- The variation of the lift and drag coefficients with angle of attack for a 5-percent-thick half-diamond-section airfoil at $M = 6.86$ and $R = 0.98 \times 10^6$.

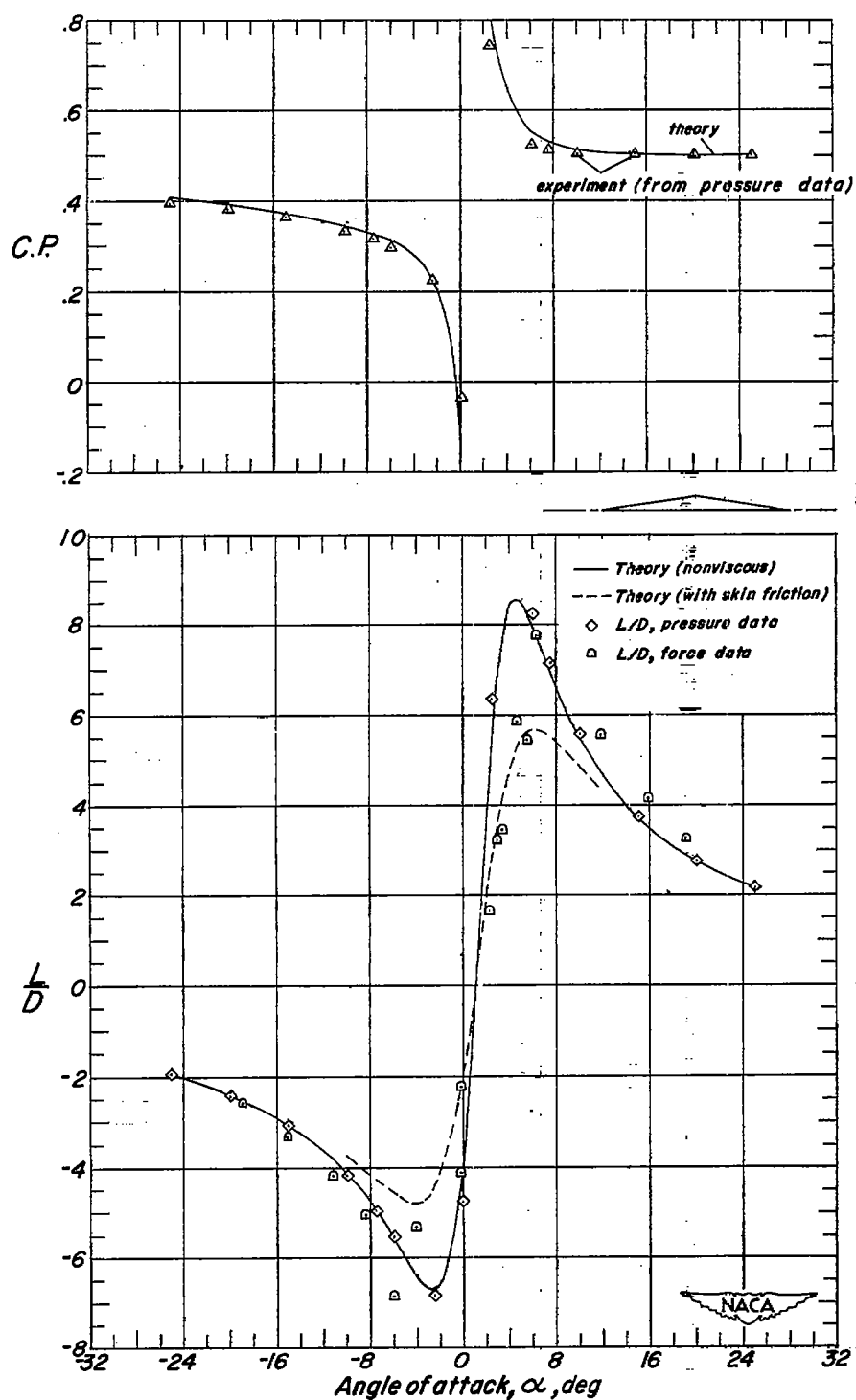


Figure 17.- The variation of the center of pressure and the lift-to-drag ratio with angle of attack for a 5-percent-thick half-diamond-section airfoil at $M = 6.86$ and $R = 0.98 \times 10^6$.

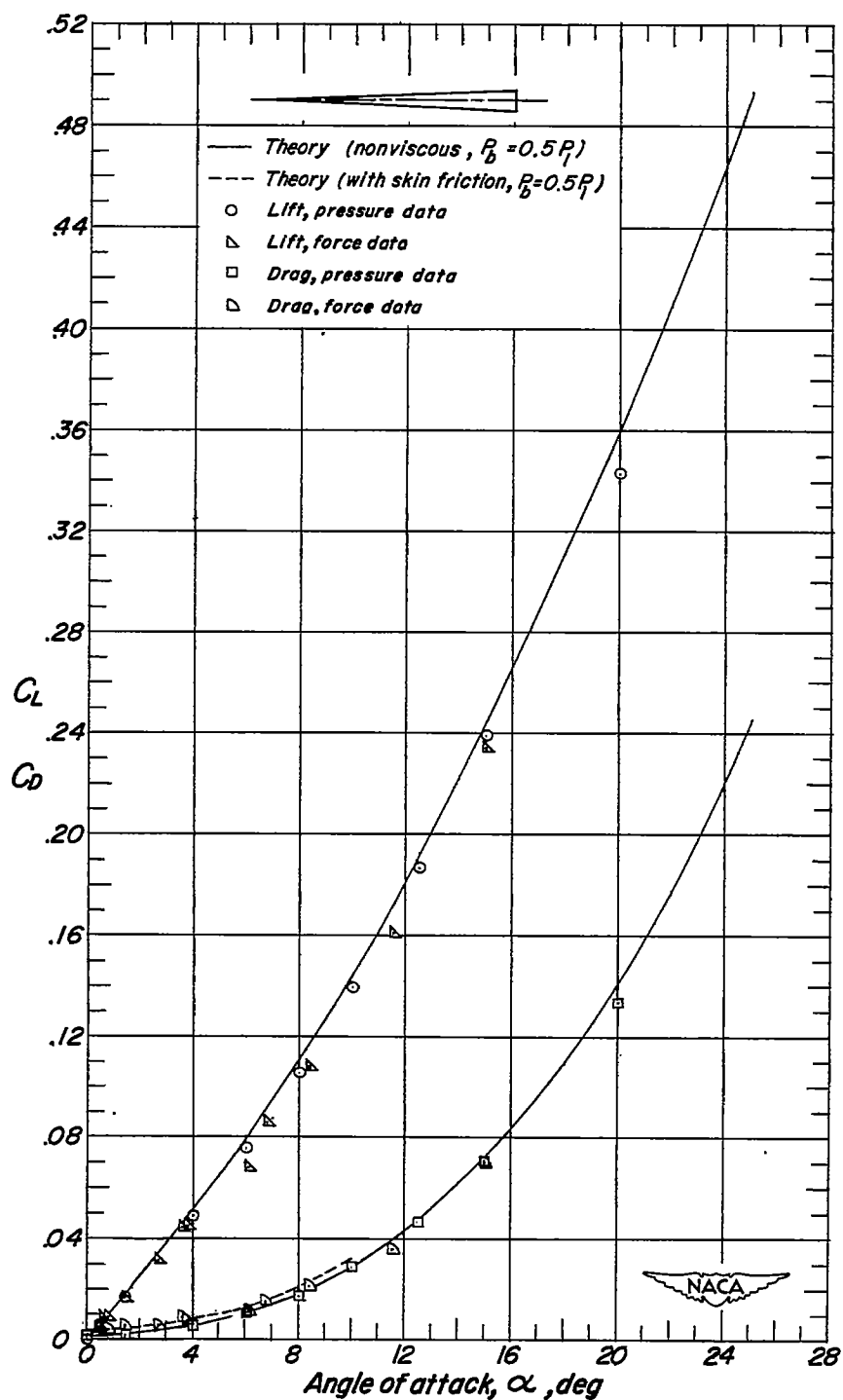


Figure 18.- The variation of the lift and drag coefficients with angle of attack for a 5-percent-thick wedge-section airfoil at $M = 6.86$ and $R = 0.98 \times 10^6$.

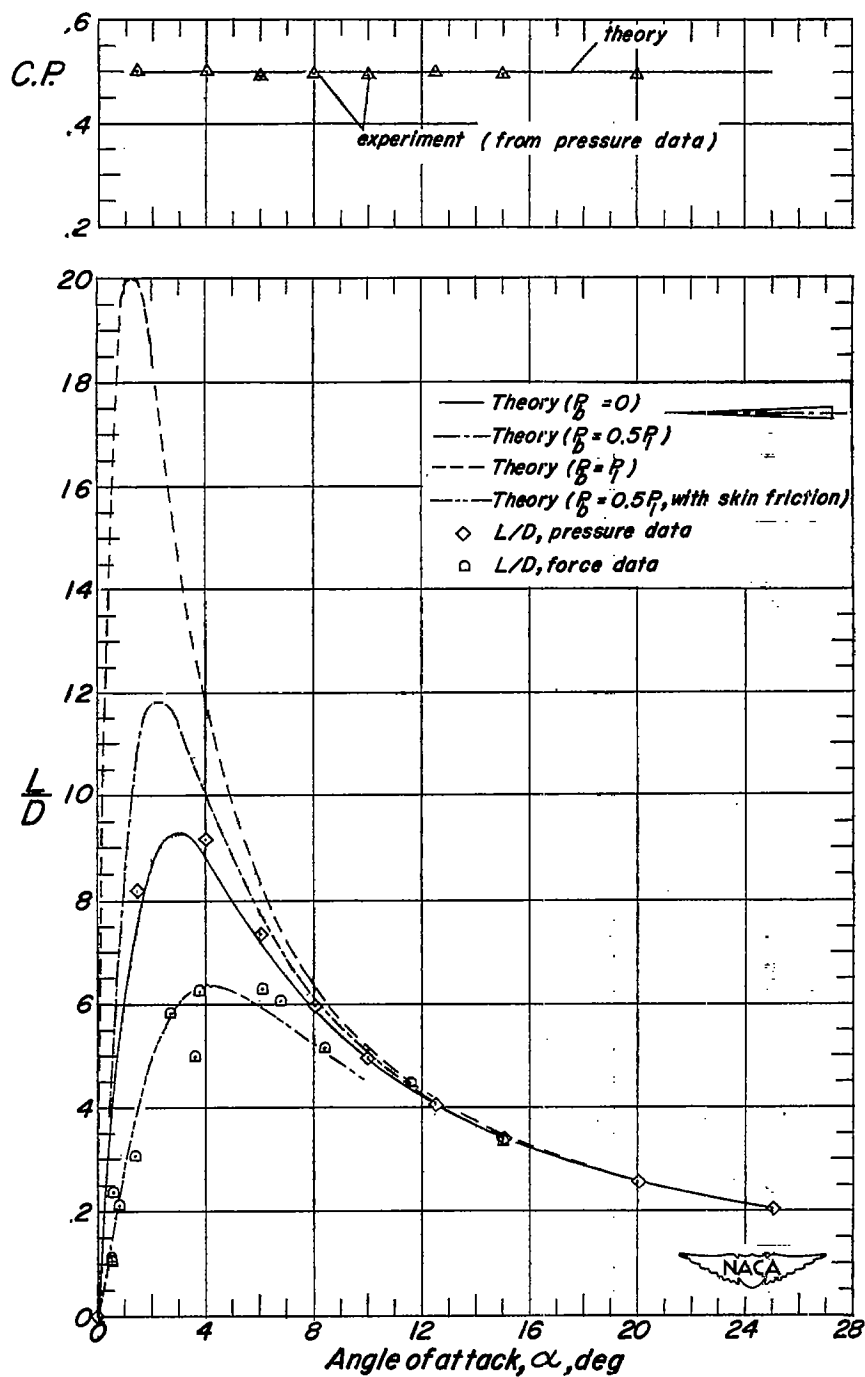


Figure 19.- The variation of the center of pressure and the lift-to-drag ratio with angle of attack for a 5-percent-thick wedge-section airfoil at $M = 6.86$ and $R = 0.98 \times 10^6$.

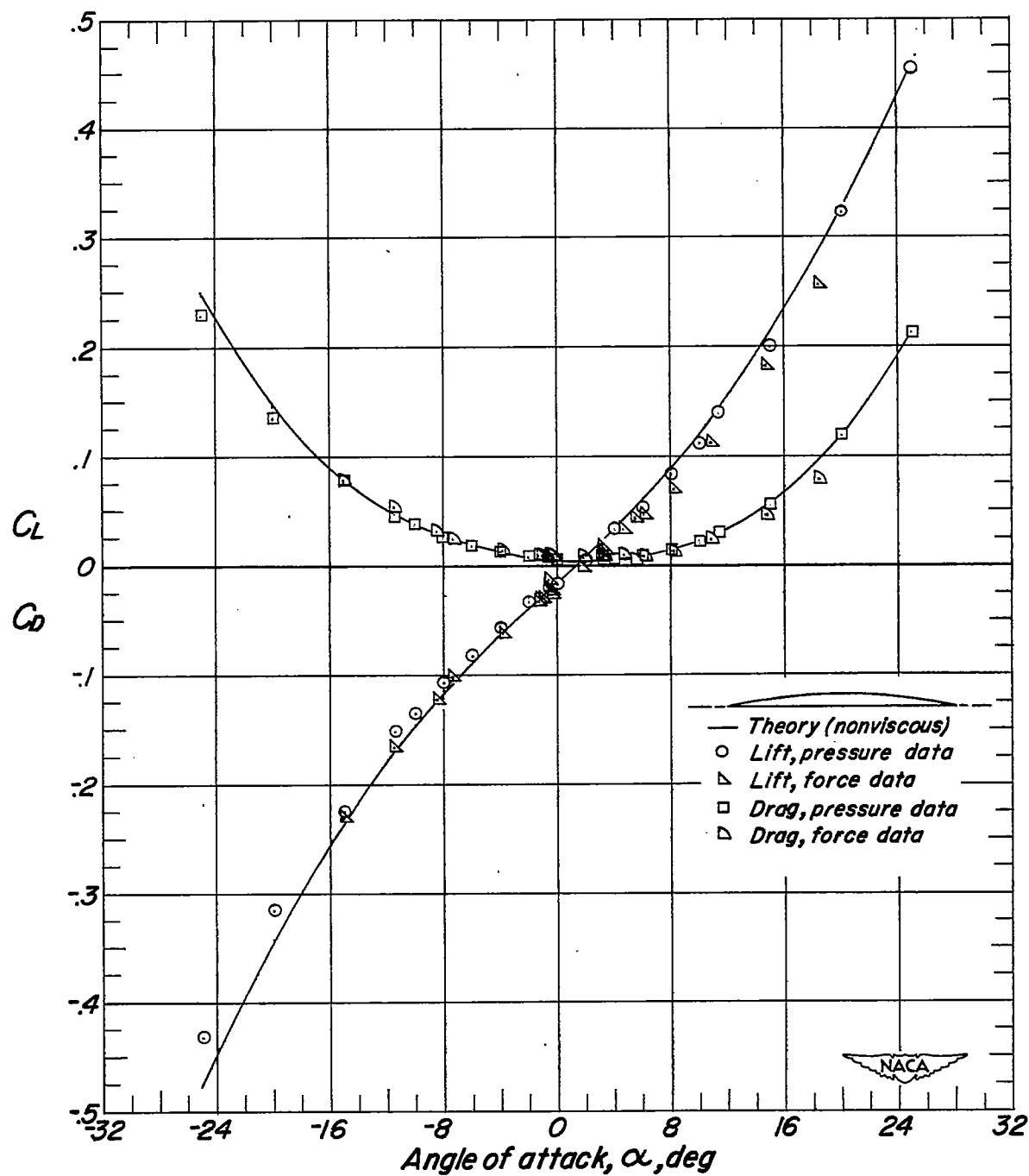


Figure 20.- The variation of the lift and drag coefficients with angle of attack for a 5-percent-thick half-circular-arc airfoil at $M = 6.86$ and $R = 0.98 \times 10^6$.

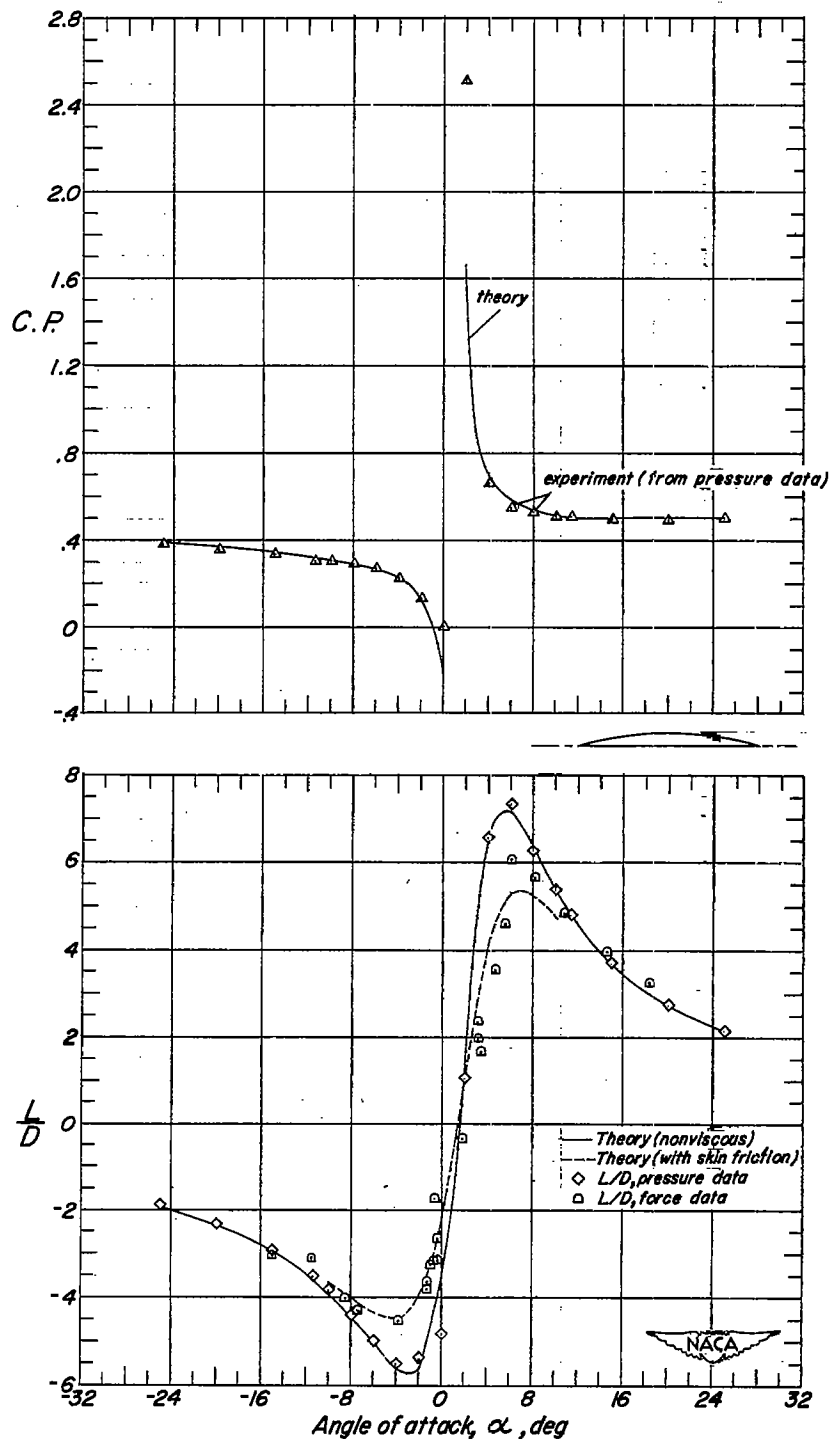


Figure 21.- The variation of the center of pressure and the lift-to-drag ratio with angle of attack for a 5-percent-thick half-circular-arc-section airfoil at $M = 6.86$ and $R = 0.98 \times 10^6$.

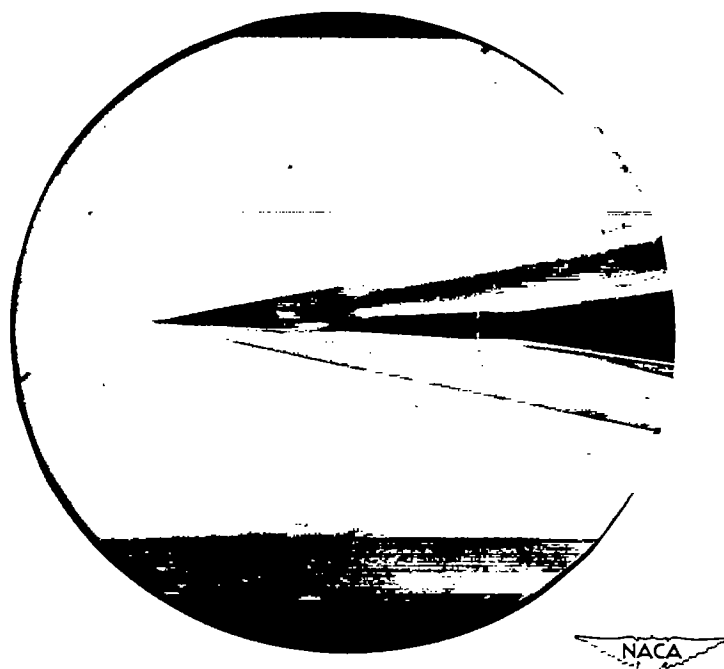
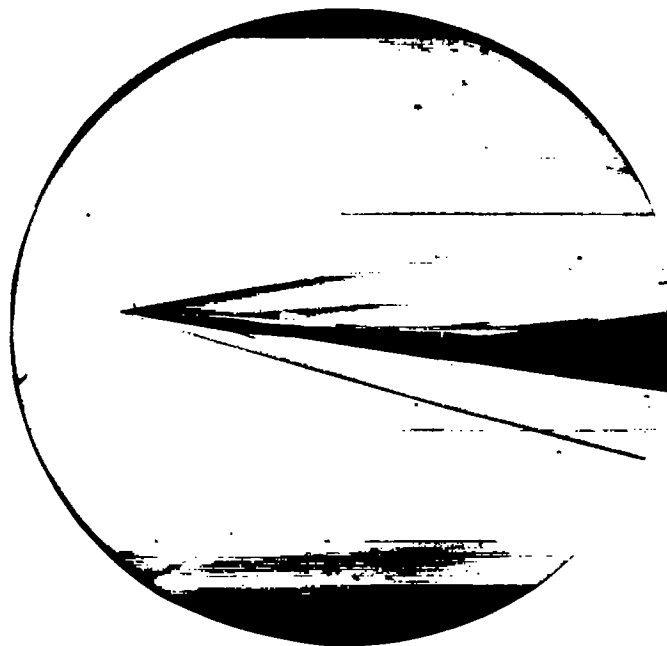


Figure 22.- Schlieren photograph of flow about a wing having a 5-percent-thick diamond section, $\alpha = 0.5^\circ$.

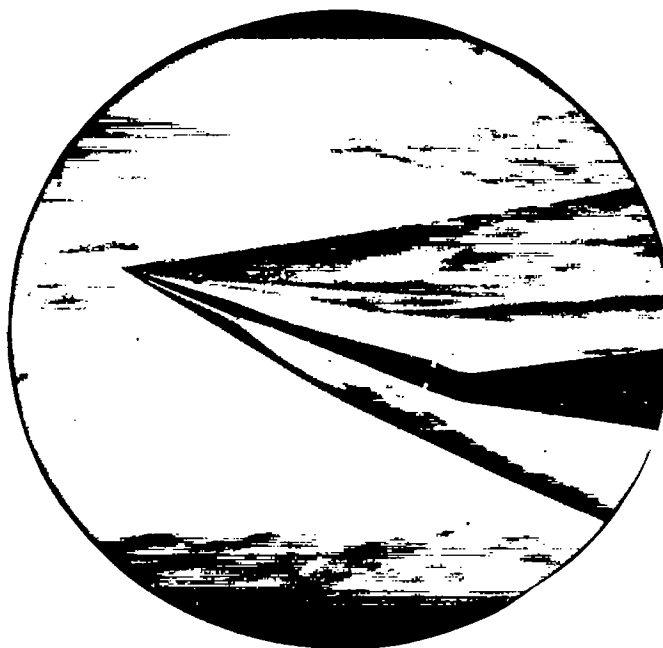


L-69126

Figure 23.- Schlieren photograph of flow about a wing having a 5-percent-thick diamond section, $\alpha = 7^\circ$.



Figure 24.- Schlieren photograph of flow about a wing having a 5-percent-thick diamond section, $\alpha = 16.8^\circ$.



L-69127

Figure 25.- Schlieren photograph of flow about a wing having a 5-percent-thick diamond section, $\alpha = 21.5^\circ$.